Computational modeling of cell sorting, tissue engulfment, and related phenomena: A review

G Wayne Brodland

Department of Civil Engineering, University of Waterloo, Waterloo, ON N2L 3G1 Canada; brodland@uwaterloo.ca

Embryonic cells have the remarkable ability to spontaneously reposition themselves with respect to other cells in an aggregate, an ability that is central to embryo morphogenesis, many disease processes, wound healing, and tissue engineering. In these rearrangements, cells of two or more histological types in a heterotypic aggregate can sort, mix or form checkerboard patterns and contacting fragments of different homogeneous tissues can spread over or engulf one another. In this article, the experimental literature on cell and tissue reorganization is summarized, the main sub-cellular structural components are identified and hypotheses about how these components interact to drive specific patterns of rearrangement are outlined. Making extensive use of tables, the article then maps out the interplay between experiments, theories, ultrastructural discoveries and computer models in the advancement of the field. The article summarizes the main computational approaches, including cell and sub-cellular lattices, body centric, boundary vertex and finite element models. The principle of operation, advantages and disadvantages of each approach is discussed, and the contributions of representative papers noted. Strong commonalities are found in the physical basis of the models and in the predictions they make. Computational models provide an important ongoing complement to experimental and theoretical studies. This review article cites 154 references.
[DOI: 10.1115/1.1583758]

1 INTRODUCTION

By what means do the cells in an aggregate reposition themselves? This fundamental question is central to many high-profile areas of biological science and medicine, including embryology, wound healing, pathology, and tissue engineering [1–4]. Answers to this question are crucial to an understanding of the causes of birth defects [1,5,6]; the mechanisms by which cell-cell organization is determined in tissues, organs, and engineered constructs [3,7,8]; and certain mechanical aspects of cancer and other diseases [3,4,9–11]. Understanding the complex sequences of mechanical interactions involved in typical cell-cell rearrangements (Figs. 1 and 2) is difficult without the use of suitable computational models.

Computational models have come to play a critical role [14,15] in biology because they provide a reliable and objective means to test hypotheses about the behavior of complex systems [6,16–18]. As a result, they have had a dramatic impact on many areas of science and medicine, including drug discovery [19], orthopedic mechanics [20,21], and biomaterials [22]. As this article will show, computational models have played a key role in the study of cell-cell interactions.

If embryonic cells of two or more histological types (heart and liver, for example) are brought into contact with each other, they can undergo spontaneous and specific patterns of rearrangement [13,23–27]. These rearrangements include sorting of cells by type, the formation of checkerboard patterns, engulfment of one cell type or tissue by another, and other distinctive geometric rearrangements as illustrated in Fig. 2. Masses of a single cell type can also undergo a number of rearrangements (Fig. 1). The cause of these self-driven rearrangements has been the subject of much research during the last four decades (Table 1), and because a wealth of different transformations can be observed and identified, these rearrangements have become a standard probe for investigating the basic mechanics of cell-cell interactions.

A discussion of cell self-rearrangement would be incomplete without mention of the remarkable fact that when the tissues of certain organisms are dissociated by mechanical or other means, they can spontaneously reestablish the form and function of the organisms [29,47–49]. One of the most notable examples of regeneration is seen in hydra, which consist of a hollow cylindrical body made of two layers of cells: ectoderm on the outside and endoderm on the inside [28,49,50]. One end of the cylinder is equipped with tentacles to facilitate feeding, while a basal disk closes the

Transmitted by Associate Editor LA Taber

other. If the tissues of one or more hydra are dissociated and allowed to reaggregate, they spontaneously form new, fully functional hydra. The process of regeneration requires several days; involves a series of steps that include sorting, formation of a hollow bilayer, and regeneration of head and foot; and incorporates differentiation as well as cell migration. Interestingly, the cells that were ectoderm in the original hydra form ectoderm in the new hydra, and the original endodermal cells form the new endoderm [51]. After reforming these two layers, the cells exhibit the distinctive cell shapes and mitosis patterns characteristic of their respective layers. That dissociated tissues can build a complete, functional organism is astonishing.

Like the processes of cell sorting and tissue engulfment, the impressive rearrangements necessary for hydra reconstruction raise fundamental questions about the mechanics of cell-cell interactions. Why do contacting cells adhere to each other? What causes cells to move relative to each other in ways that have meaning on a global scale (eg, the process of sorting)? Is it possible to determine the mechanical *rules* that govern these interactions? Can these rules be explained in terms of the structural components of the cell? Is it possible to verify hypothesized explanations using computational simulations or other means? Can the rules or parameters used in computational simulations be modified so as to obtain new insights into the mechanics of cell-cell interactions? These are the issues with which this review is concerned. Although the process of discovery has involved considerable interplay among experiments, theory, and computational modeling (Table 1), special attention is given here to computational models and the insights that they have provided.

A number of terms are used in a specific technical sense throughout this work, and are identified in this and the following paragraphs of this section by italic font. A *cell mass* is an aggregate of embryonic cells. If two or more cell *types* are interspersed with each other, the mass is termed *heterotypic* (Fig. 2), while a cell mass consisting of only one cell type is called *homotypic* (Fig. 1). Two or more homotypic masses or *tissues* may be brought into contact with each other in order that they may interact with each other. Phenomena that occur include *sorting*, *mixing*, and formation of *checkerboard* patterns in heterotypic aggregates (Fig. 2) and *engulfment, separation*, and *dissociation* of tissues (Fig. 1). One objective of studies of cell-cell interactions is to determine the necessary and sufficient *conditions* for each of these phenomena. Cells become functionally and histologically different from each other through a process called *differentiation*. Two cell types of interest here are *epithelial* cells, which form confluent layers, and *mesenchymal* cells, which form loosely organized 3D masses.

A cell mass, or a model of it, is assumed to begin from a so-called *initial configuration*. Each follows a *path* through *configuration space* that consists of a *sequence* of *incremental* geometric changes. Ultimately, each reaches a *final configuration* in which small oscillations in geometry may occur, but from which substantial further changes would not occur. Cell-cell interactions are understood to be driven by mechanical *forces* that derive from the *physical properties* and structure of the cells; these forces may arise from *thermodynamic* considerations. *Chemotaxis* is directed cell movement that results from specific cell actions in response to external chemical gradients. The chemical signals do not themselves apply a force to the cell, although they may induce the cell cytoskeleton to undergo specific patterns of force production that are similar in effect to forces produced by other causes. The path taken through configuration space is that which minimizes an *objective function* such as *system free energy*. The final configuration may correspond to a *local minimum* in the free energy surface rather than its *global minimum*. Energy may be lost to viscous and other effects through a process called *dissipation*. Depending on how a model is formulated, its path through configuration space may corre-

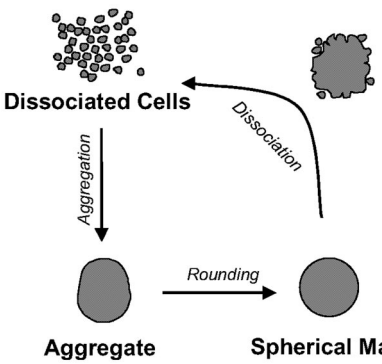

Fig. 1 Classifications for homotypic systems of cells: Under suitable conditions, dissociated cells join together to form an aggregate which typically reshapes into a spherical mass. If suitable changes are made to the medium (see [12]), the cells on the surface of the mass will dissociate from the rest of the mass until, ultimately, all of the cells become dissociated from each other.

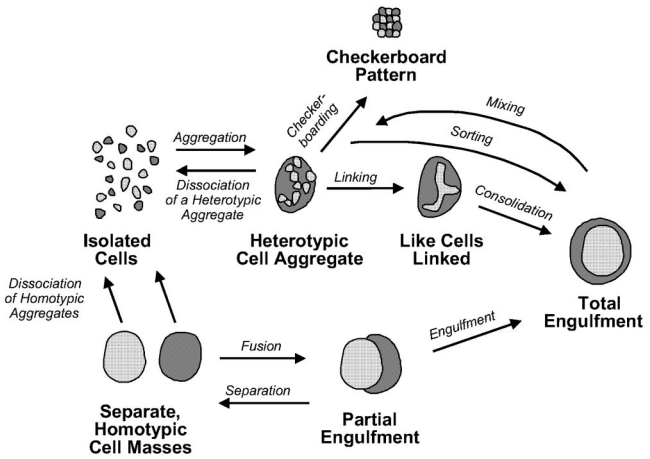

Fig. 2 Classifications for heterotypic systems of cells: Many states are possible when two cell types are present. Under suitable conditions, two separate homotypic masses can fuse together, with one partially or totally engulfing the other. Alternatively, isolated cells of these same two types can aggregate, sort and produce a final state that is similar to that produced by engulfment. Other possibilities include the formation of checkerboard patterns. Reprinted from [13].

Table 1. Overview of the historical relationship between experiments, theories, ultrastructural discoveries and computational models: Contributions are reported according to the approximate time that they first impacted the study of cell-cell interactions. Representative references are shown.

Time Period	Experiments	Theories	Ultrastructure	Computer Models
1700s	Early experiments on sponges [28]			
1900s	Reconstitution of sponges [29]			
1940s	First proof that motions in reconstituted aggregates are governed by original histological typing of cells [30]			
1950s	Studies of aggregates [31]			
1960s	Systematic studies of different cell-cell combinations [12,23,25,32–34]	Differential Adhesion Hypothesis (DAH) [12,23,32–34]		
1970s	Role of microfilaments [35]	Differential Surface Contraction Hypothesis and other hypotheses [36,37]	Microfilaments, microtubles and other sub-cellular components [38,39]	Cell Lattice Models [40,41]
1980s			Cell adhesion molecules (CAMS) [42]	Centric Models [43,44] Vertex Models [45]
1990s	Role of CAMs [42]			Sub-cellular Lattice Models [27]
2000s		Differential Interfacial Tension Hypothesis (DITH) [13]		Finite Element Models [46]

late directly with *time*. If not, a *pseudo-time*, based on the number of *iterations* of the *algorithm*, may be used.

The system free energy is assumed to depend on a physical property that is constant per unit of *boundary* that occurs between each pair of contacting cells or between a cell and a surrounding liquid *medium*. Although this property has often been associated with *cell-cell adhesion*, it has been shown recently that the governing property is the net *surface tension*, or more precisely *interfacial tension*. Model input values such as force, pressure, and size are typically handled using *parameters* that are cast in *dimensionless* form.

2 FORCES THAT DRIVE CELL-CELL INTERACTIONS

If computational models are to be biologically meaningful, they must be based on the forces that drive cell-cell interactions and they must address theories about how these forces interact.

2.1 Structural overview

The eucaryotic cell [52,53] (Fig. 3) is a highly sophisticated and impressive entity [17,54], far surpassing even the most advanced systems designed by humans. Current knowledge regarding the structure and function of cells would fill many volumes, and is beyond the scope of this review. However, an understanding of the cell-cell interactions of interest in this review requires a basic knowledge of those components of the cell that may be involved in these interactions. Since the cell-cell interactions of interest in this review are caused by the surface properties of cells, the focus of this section is on those structures that influence surface properties.

The cell is a discrete entity that typically has dimensions in the range of 5–100 μm and is bounded by a bilayer lipid membrane. This membrane contains pumps, channels, receptors, ligands, adhesion molecules, and other specialized

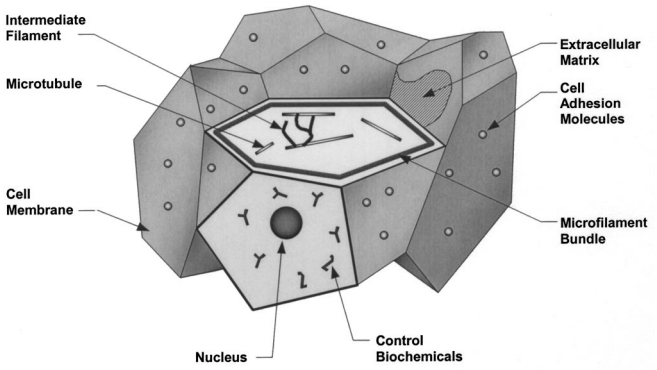

Fig. 3 Schematic of cells in a 3D aggregate: The forward-most cell has been sectioned to reveal the nucleus and control biochemicals, some of which it responds to and others of which it produces. The upper-most section through the same cell shows primary structural components, including microfilaments along the inner surface of the cell, and microtubules and intermediate filaments that are present in the cytoplasm that fills the cell volume. Also shown are the extracellular matrix (ECM) and cell adhesion molecules (CAMs) that act between the cells.

structures (Fig. 4). These membrane-bound proteins evidently maintain the chemical balances and the electronegativity of the cell, and allow it to communicate with adjacent cells, to sense cell deformation, and to transmit forces from one cell to another. A number of internal structures—including the smooth and rough endoplasmic reticula, the Golgi apparatus, lysomes, and peroxisomes—are considered to form part of this membrane system. The membrane and its associated structures vary significantly from one cell type to another, but they have been shown to generate tension in the plane of the membrane and to cause the membrane to exhibit viscoelastic tensile and bending properties. At the relatively low strain rates characteristic of the movements of interest here, these membranes and their associated structures are assumed to generate an in-plane tension F_{Mem} that is constant. As the membrane stretches or contracts, lipids and other materials are evidently manufactured or taken back into the cell as needed. In present models, the time constants of the shape changes are assumed to be sufficiently long compared to those of the manufacturing and resorption processes that F_{Mem} remains constant.

Residing in the membranes of many cells are one or more types of cell adhesion molecules (CAMs) [52,55–60]. These structures bind to each other, to the extracellular matrix (ECM), and to various substrates (Fig. 4). Cell-cell and cell-substrate adhesion systems come in many varieties, some of which utilize the same adhesion molecules on adjoining cells (called a homotypic interaction) and others which involve complementary molecules (a heterotypic interaction) [59]. CAMs have been directly implicated in cell sorting [42,61–66]. In most current models, CAMs are assumed to generate a constant per unit of cell contact area, while the magnitude of this force is assumed to depend on the cell types that form the interface. This assumption would be appropriate if CAM-CAM interactions are thermodynamically reversible, if CAMs occur and remain uniformly distributed on the cell surface, and if there are a sufficient number of CAMs to maintain smooth surface-surface interactions.

It can be shown that the normal force caused by cell-cell adhesion is equivalent to a force F_{Adh} tangential to the interface [46,67]. This force tends to cause the boundary between the cells to increase in area because chemical energy is released as the CAMs or other surface molecules come into contact and bind with each other. Thus, the mechanical effect of CAMs is opposite to that of the in-plane tension generated by the cell membrane. An equivalent force can be used even in cases where binding is time dependent [68] or expends metabolic energy [69]. In these cases, F_{Adh} becomes a function of time and whether the edge of the interface is advancing or receding. As the specifics of particular adhesion systems become more completely characterized and the forces they produce are measured [70–73], F_{Adh} can be written as a function of the concentrations of the relevant cell surface molecules and their medium-borne regulators. In present computational models, F_{Adh} is assumed to be constant at each interface, but to depend on the types of the cells that form that interface.

Inside the cell, the most conspicuous organelle is the nucleus. It is surrounded by a membrane system that separates the genetic material contained therein from the rest of the cell. This genetic material contains the instructions necessary to construct the cell and its components (mitochondria contain additional DNA, and certain structures, such as centrosomes, are produced epigenetically), and to regulate the operation of these components through a complex sequence of biochemical pathways. Other organelles inside the cell include mitochondria, important for cell metabolism, and a variety of structural elements known as cytoskeletal components.

Cytoskeletal components are primary structural elements in the cell and include microfilaments, microtubules, and intermediate filaments (Fig. 3). It is difficult to make generalizations about the structure and function of these components since they serve such a broad range of mechanical functions and occur in a vast array of geometrical configurations. However, in terms of cells that are in aggregates, microfilaments tend to organize along the inside of the cell membrane [38,74–76] and are understood to contribute a tension F_{MF} parallel to the cell surface [37]. Exposure of a cell surface to a medium causes the formation of microfilaments along that surface, and an increase in surface contraction [39]. The forces generated by microfilaments are important for cell sorting [35,42]. Other components of cell systems that may be involved to a greater or lesser extent in the cell-cell interactions of interest here include desmosomes, gap junctions, the extracellular matrix (ECM), microtubules, and intermediate filaments.

Although traditional views of the cell imply a rather sparse arrangement of cytoskeletal components, contemporary views suggest that they are quite densely packed and that the mean distance between protein structures may be as small as six times the thickness of a layer of water molecules [54,77,78]. From a mechanical perspective, these extensive

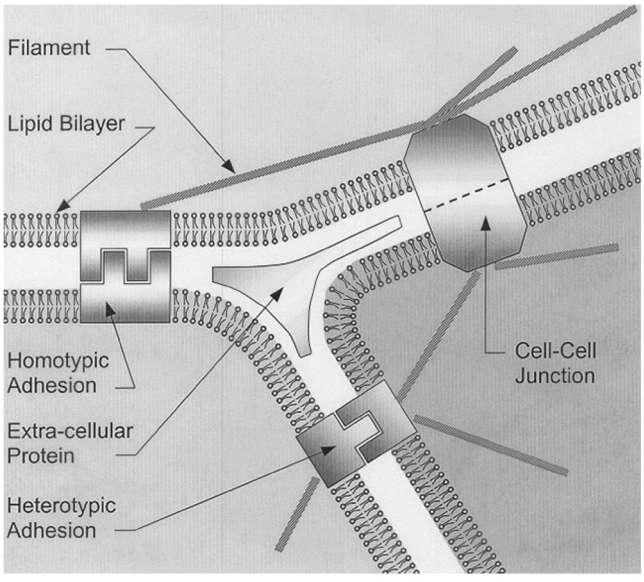

Fig. 4 Schematic of a close-up view of the triple junction between cells: Three cells (shown lightly shaded) contact each other. The bilayer membranes along the edges of the cells are shown, as are two kinds of cell-cell adhesion systems and a cell-cell junction.

networks give the contents of the cell a relatively high effective viscoelasticity and play a key role in mechanotransduction. Since the networks are labile at low strain rates, like those characteristic of the self-rearrangement of cells, the cell cytoplasm and its associated networks are assumed to exhibit an effective viscosity μ [46,79]. The liquid component of the cytoplasm generates a hydrostatic pressure that balances the tensions produced along the cell surfaces and thereby maintains the volume of each cell.

The geometric arrangement of the cytoskeleton differs greatly depending on whether cells are individually plated on a substrate, form a confluent monolayer, or are in a 3D mesenchymal cell aggregate. In the first case, the cells form focal adhesion plaques and stress fibers. In the second, actin forms a cylindrical cortex, and CAMs are distributed essentially uniformly on the lateral surfaces of the cell. In the third case, the actin forms a polyhedral shell, and CAMs are distributed approximately uniformly over the surface of the cell.

During early embryogenesis, cells become functionally different from each other through a process called differentiation [52]. Although the means by which this occurs is not completely understood, it is known that differentiation causes the cytoskeleton, CAMs, genes, and many other key components of the cell to demonstrate type-specific characteristics. These distinctive characteristics give rise to type-specific mechanical properties and ultimately drive the intriguing cell self-rearrangements shown in Figs. 1 and 2.

Although the structural model of the cell presented here is highly simplified, it is sufficient for explaining the basis and limitations of current theories and computational models of cell-cell interactions.

2.2 Functional overview

In this paper, the cell is assumed to operate in a mechanistic fashion through a complex interplay of biochemical, mechanical, and electrical factors [52,80]. The physical conditions shown on the left of Fig. 5 can be thought of as input variables with respect to a model of the cell. These variables affect the cell by means of specialized structures such as channels and receptors in the cell membrane. Then, specific changes in the state or action of the cell are brought about through complex pathways that may have biochemical or mechanical components. The nucleus may or may not be directly involved in all of these pathways, although it sets up the conditions for their operation. Ultimately, as a result of these internal actions, the cell may release biochemicals, change shape, or lay down ECM. These actions can be considered output variables that result from the cell's processing of the input variables. The input-to-output process may involve the entire cell or just a small portion of it.

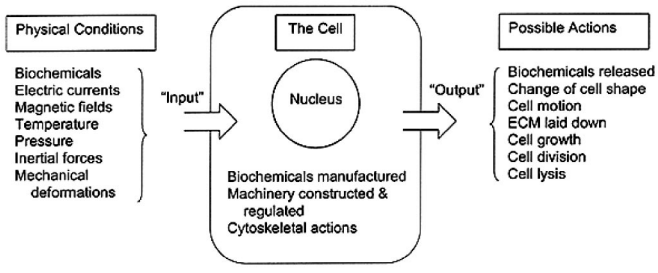

Fig. 5 Functional model of the cell: The cell is understood to take certain ''input'' and to respond by producing certain *output*.

The fields of biomechanics and mechanobiology have done much to advance a mechanistic mode of thinking. They have also led to the mindset that all cell actions and interactions can ultimately be explained in terms of principles of chemistry and physics, and that to be valid, explanations must be consistent with these principles. One consequence has been the reintegration of the three traditional branches of science: chemistry, physics, and biology.

Although assumptions must often be made before research can begin, it may be difficult to revisit those assumptions objectively. As a result, new findings are often interpreted in terms of preexisting theory [81], and the catalyst for a paradigm shift must often come from a new approach. Computational models have played precisely this role in the investigation of cell-cell interactions.

2.3 Surface tension and surface energy

If two isolated cells, labeled *A* and *B* in Fig. 6*a*, are brought into contact with each other (Fig. 6*b*), several approaches can be taken to interpret the mechanics of this process. The free energy per unit area of *A*-medium interface is called W_{AM} while the energies associated with the *B*-medium and *A*-*B* interfaces are called W_{AM} and W_{AB}, respectively. At any instant in time, the contribution to the system free energy from these interfaces is

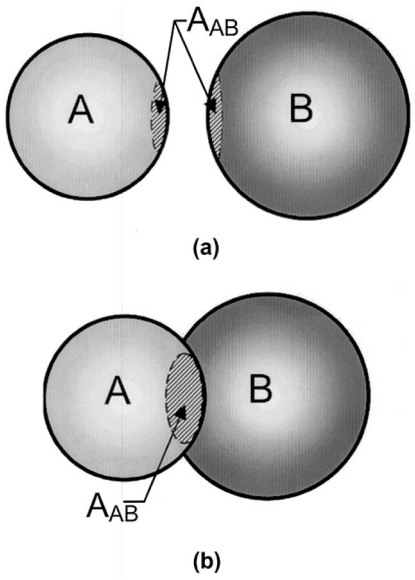

Fig. 6 Contact of two isolated cells: Two isolated cells *A* and *B*, as shown in part *a* of the figure, are brought together *b*. During this process, surface regions of approximate area A_{AB} on each cell come into contact with each other to form a new interface, also approximately of area A_{AB}. As each new unit area of *A*-*B* contact is produced, approximately a unit area of *A*-*M* (medium) interface and a unit area of *B*-*M* interface are lost.

$$W = A_{AM}W_{AM} + A_{BM}W_{BM} + A_{AB}W_{AB} \quad (1)$$

where A_{AM}, A_{BM}, and A_{AB} are the areas of the *A*-medium, *B*-medium, and *A*-*B* interfaces, respectively.

Mechanical systems that have surface or interfacial tensions also have interfacial energies that are proportional to the products of their interfacial tensions and the areas over which each acts. Thus, the interfacial energy density W associated with each interface might be interpreted as an equivalent surface tension γ [67], where

$$W_{AM} = \gamma_{AM} \quad (2)$$

Brodland *et al* [13,82,83] have previously espoused an interpretation of surface energies in terms of interfacial tensions and calculated an equivalent surface tension directly from the forces generated by various subcellular components discussed in Section 2.1. For an interface between two cells of types *A* and *B*, the equivalent interfacial tension γ_{AB} is

$$\gamma_{AB} = F_A^{Mem} + F_B^{Mem} + F_A^{MF} + F_B^{MF} - F_{AB}^{Adh} + F_{AB}^{Other} \quad (3)$$

where F_A^{Mem} and F_B^{Mem} are the strengths of the tensions in the membranes on the surface of the type-*A* and type-*B* cells, respectively; F_A^{MF} and F_B^{MF} are the strengths of the equivalent contractions along the surface of the cells due to contraction of microfilaments and the actions of other cytoskeletal components; F_{AB}^{Adh} is the equivalent expansive force due to cell-cell adhesion; and F_{AB}^{Other} is the net surface contraction from any other factors incorporated into the model. In the case of a cell-medium interface, Eq. (3) is modified to

$$\gamma_{AM} = F_A^{Mem} + F_A^{MF} - F_{AB}^{Adh} + F_{AB}^{Other} \quad (4)$$

where F_{AB}^{Adh} is a generalization of the adhesion concept.

The equivalent interfacial tensions given in Eqs. (3) and (4) are not quite the same as the interfacial tensions that act along interfaces with fluids. When an interface involving a fluid has a positive interfacial tension, the fluid molecules at the interface have a higher free energy than do those that are inside the fluid and surrounded entirely by like molecules. If the interface is with another fluid, all molecules at the surface of the first fluid try to move further into their own fluid so as to minimize their individual free energies. The result is a local self-leveling of the surface, which can be shown to have the same mechanical effect as a tension along the interface. Hence, the concept of an interfacial tension in fluids. In the case of a liquid, this force is constant under ordinary rates and degrees of surface expansion or reduction because an ample supply of molecules is readily available to form new surface or to fully encapsulate molecules no longer needed at the surface.

At the surface of a cell, the degree and rate of surface expansion or reduction are presumably affected by cell manufacturing and adsorption processes and by factors associated with cytoskeletal remodeling. In present models, these rates are assumed to be sufficiently high that the net interfacial tension does not change. Should details of force variation in the cell surface expansion or contraction rate become available, the interfacial tension could be made rate dependent.

The interfacial tension at a certain location on the surface of a cell could also be affected by in-plane motion of cell-cell adhesion molecules. The concept of a constant (negative) contribution F_{AB}^{Adh} to the interfacial tension γ assumes that the density of the adhesion molecules is uniform over the surface of the cell and that the density does not change as the cell deforms. If the contact area between two cells decreases, does the number of adhesion molecules on that surface reduce proportionately? Does the cytoskeleton remodel in such a way during this process that it maintains a uniform density of adhesion molecules at every location over the cell surface? It seems unlikely that the answers to these and other relevant questions would support the concept of a constant effect of cell-cell adhesion on interfacial tension. However, experiments indicate that the tension at the interface between cells in a mass and the surrounding medium remains constant as the mass and its cells are deformed [84,85]. Thus, the concept of a constant equivalent surface tension appears to be justified.

An advantage of an interfacial tension approach is that it lends itself to direct physical interpretation, to force vector techniques, and to the finite element method. However, the term interfacial tension in the context of cell-cell interactions is intended to embody the net tension that acts along cell-cell and cell-medium interfaces. It is not intended to explicitly embody all of the subcellular complexities of the cell nor to imply the availability of a virtually unlimited amount of boundary, as is the case with fluids.

An alternative to the use of interfacial tensions is to focus on the differences in the energies associated with various interfaces. If that approach is taken, one less parameter is needed to describe a system of cells. However, to realize this advantage, one is required to manually choose an interface as the reference, and the original surface energies cannot be recovered [27].

Another look at the two cells brought into contact in Fig. 6 reveals that, if the area of the newly formed interface were ΔA_{AB}, then the contact area between each of the cells and the surrounding medium would be reduced by approximately ΔA_{AB}. If each interface in the system has a free energy W per unit area associated with it, then the change ΔW in the free energy of the system will be given by

$$\begin{aligned} \Delta W &= \Delta A_{AB}(W_{AB} - W_{AM} - W_{BM}) \\ &= \Delta A_{AB}(\gamma_{AB} - \gamma_{AM} - \gamma_{BM}) = -\Delta A_{AA}W_{A\text{-}B} \end{aligned} \quad (5)$$

where $W_{A\text{-}B}$ is the negative of the reversible work of adhesion or bond energy, associated with *A*-medium and *B*-medium interfaces being replaced by the same amount of *A*-*B* interface. Although $W_{A\text{-}B}$ is sometimes called surface tension and is represented by the symbol γ [27] (in some cases it is given the opposite sign to that used here), it does not correspond to the surface tensions used herein. If the work of adhesion is positive, cell-cell interfaces have less free energy than cell-medium interfaces and would occur preferentially. Thus, type-*A* cells in contact with type-*B* cells would aggregate.

A strict accounting of surfaces gained and lost reveals that the medium that had formed *A*-medium and *B*-medium interfaces, each of area ΔA_{AB}, might now be considered to form a new virtual medium-medium interface with a total area of ΔA_{AB}. Equation (5) tacitly assumes that the tension (and energy) associated with this medium-medium boundary is zero. Should the medium-medium interfacial tension or its analogue in a particular system not be zero, W_{AM} could be adjusted to account for an appropriate loss of virtual medium-medium boundary. If cells *A* and *B* are of the same type,—*A*, for example—then the change in free energy released by the formation of that type of homotypic interface is

$$\Delta W = A_{AB}(W_{AA} - 2W_{AM}) = A_{AB}(\gamma_{AA} - 2\gamma_{AM}) = -\Delta A_{AA} W_{A\text{-}A} \tag{6}$$

where $W_{A\text{-}A}$ is the negative of the reversible work of cohesion. Unfortunately, the definitions, signs, and notations used for $W_{A\text{-}A}$ and other relevant quantities vary widely from author to author [27,67,83,84]. The author of this article recommends the indicial convention of Glazier and Granger [27] for identifying boundaries, calling the surface tension produced by a cell of type *A* in contact with the medium γ_{AM}, rather than $\gamma_{A\text{-}A}$. The benefits of this approach are especially evident when three or more cell types are present. The author of this article is also partial to using interfacial tensions rather than works of adhesion because the former leads to an understanding of the way force imbalances cause triple junctions between cells to move and of the reasons why these motions accumulate to produce sorting and envelopment.

2.4 Hypotheses regarding how cell rearrangements are driven

Early experiments provided important information regarding the motions of cells in aggregates [28,29,31,86–88] and initiated the development of theories to explain these motions. Although these theories have bases ranging from energy concepts to the actions of specific ultrastructural components, all focus on the forces that act at or near the cell surface. The theories are grouped into four categories.

2.4.1 Differential adhesion hypothesis (DAH)

A number of theories of cell sorting are based on the concept of cell-cell adhesion. The basic idea behind this intuitive concept is that cells tend to contact certain cell types rather than others due to type-specific strength-of-adhesion differences between them. The earliest version of this theory proposed that cell sorting could be explained in terms of selective intercellular adhesion [88].

This proposal was followed by a series of clever and systematic experiments by Steinberg and others [23–25,32–34,85,89–92] to investigate cell and tissue interactions. Some of the earliest of these experiments showed that tissues and immiscible liquids behave in similar ways. In the case of liquids, sorting and engulfment are driven by differences in the intermolecular attractions among different types of molecules [93]. Could cell and tissue motions be driven by corresponding differences in the adhesion between different types of cells?

These experiments ultimately led to the formulation of the Differential Adhesion Hypothesis (DAH) [12,23,32–34,89], or Steinberg Hypothesis [37]. The DAH states that [26] *i*) cells adhere to one another, *ii*) the strength of the adhesion varies from one cell type to another, and *iii*) an aggregate of cells will tend towards that configuration which minimizes the free energy of the system. The theory is general, not making reference to any specific ultrastructural components, and it is consistent with the concepts of liquid interactions. With the subsequent discovery of the molecular bases for various cell adhesion systems [55–60], the DAH became established as the *de facto* paradigm for experiments with and computational models of cell-cell interactions.

The DAH predicts [12] that if cells of two histological types are mixed, the cells with the stronger adhesion will group together and that they will be partially or totally surrounded by a mass or layer of the less cohesive cells. The same final state is predicted for tissues brought into contact with each other. However, in the case of fluids [89], the engulfment characteristics can be influenced by the relative strengths of the adhesion between the engulfed and engulfing fluids.

In 1976, Harris [37] raised a number of issues regarding the DAH. His carefully written paper identified four fundamental differences between cells and liquids. It also presented a number of alternative explanations, including the Differential Strength of Adhesion Hypothesis and the Differential Mobility of Adhesion Hypothesis to explain the available data. This paper opened the door for other challenges to the DAH [13,83]. Even though some recent interpretations of the DAH [85] are written in terms of actual surface tensions, it is difficult to reconcile the latter with the original differential adhesion concept.

2.4.2 Differential surface contraction hypothesis (DSCH)

Harris [37] enunciated a Differential Surface Contraction Hypothesis (DSCH) to explain cell-cell interactions. The DSCH assumes that *i*) cells exhibit surface contractions; *ii*) the strength of these contractions is greatest when a cell is in contact with the medium, is less when it contacts a cell of another type, and is least when it contacts a cell of the same histological type; and *iii*) cells of different types exert different degrees of surface contraction when they contact the medium. Thus, if an interface shortens by surface contraction, particles sprinkled along the initial boundary would be spaced more closely following the contraction. This situation contrasts with the DAH, where a boundary held together by cell-cell adhesion would be shortened if a portion of its apposed surfaces were pulled apart. In that case, particles sprinkled along the initial boundary could maintain their original spacing on the part of the interface that is left intact, while over the separated part of the interface, some of the particles would presumably adhere to each side of the opened interface.

The DSCH predicts cell interactions that are similar to those that would occur in immiscible fluids. Thus, it predicts

that for cells of type *A* to be drawn over those of type *B*, the type *A*-medium interface must contract strongly enough to overcome the resisting forces of the *A*-*B* and *B*-medium interfaces. The existence of contractile structures along the inside of the cell and the fact that cell-cell interactions can be temporarily stopped by the short-term application of cytochalasin *B* support this theory. However, because sorting can continue in at least one cytochalasin *B*-treated system [94], the DSCH does not provide a complete explanation of the available data. These experiments are difficult to interpret, however, because cytochalasin *B* also disrupts the attachment between actin fibers and CAMs and thus changes a number of cell properties. As noted by Harris [37], it is difficult to distinguish between the actions of surface contractions and interfacial tensions because they produce similar results.

2.4.3 Specific CAM-based hypotheses

As the surface structure of the cell was investigated in more detail, it became apparent that a number of families of cell adhesion molecules (CAMs) existed [55–60,95]. The discovery of these families gave rise to a number of investigations into the role of the extracellular matrix (ECM) [61] and the role of specific CAMs and other surface structures in the sorting behavior of cells [36,42,63–66,96,97]. These studies show that cell sorting and other types of cell-cell interactions are dependent on the nature and concentration of specific surface structures. This finding further supports the concept that cell-cell adhesion plays an important role in cell-cell interactions. The conceptual contribution of CAM-based investigations is that they allow the strength and temporal characteristics of cell-cell adhesion to be explained in terms of specific systems of surface molecules. This contribution is important because it provides a biochemical basis for differences in the strengths of cell-cell adhesion and for the selectivity of adhesion.

2.4.4 Differential interfacial tension hypothesis (DITH)

The most recent hypothesis for cell-cell interactions, and the first one to be the direct result of computational modeling, is the Differential Interfacial Tension Hypothesis (DITH). When Brodland and Chen were developing computer code for a new, cell-level finite element formulation [46], they needed a cell-level phenomenon on which to test their code. Since the phenomenon of cell sorting seemed to be well understood and adequately explained by the DAH, it was chosen as a benchmark. However, it soon became apparent that the model was in conflict with the DAH [83]. Further investigation revealed that the predicitions of the finite element model were consistent with the behavior of fluids and that discrepancies existed between the DAH and the physics of surfaces [13,82]. The model predictions were also consistent with compelling experimental evidence that engulfment is governed by surface tension [65,84,85,91].

The finite element formulation of Chen and Brodland [46] made use of the standard concept of equivalent forces, resolving the forces generated inside an element into equivalent forces at its nodes [97–99]. In the case of their cell model, the forces generated inside the cell were resolved into equivalent tensions along the boundaries of the cells. This force was complemented by an equivalent internal pressure in each cell that acts normal to these boundaries and that maintains cell volume. These boundary tensions are equivalent to an interfacial tension. Differences in the values of these tensions along specific types of cell-cell and cell-medium interfaces were found to be sufficient to explain the wide range of aggregate phenomena shown in Figs. 1 and 2. The result of these findings was the Differential Interfacial Tension Hypothesis.

The basic tenets of the DITH are that *i*) interfacial tensions act along cell-cell and cell-medium boundaries, *ii*) the value of these tensions depends on the cell or medium types that form the interface, and *iii*) these tensions cause local displacements of the triple junctions and ultimately lead to specific patterns of cell rearrangement.

The DITH involves elements of a number of other hypotheses. In particular, like the DAH, the DITH accounts for the effect of cell-cell adhesion, but it makes the important observation that cell-cell adhesion would tend to elongate boundaries. Thus, if cell-cell adhesion were sufficiently high compared to the contractions provided by other cellular components, the interfacial tension would be negative, and convoluted (jigsaw puzzle shaped) boundaries [95], like those that occur at fluid-fluid interfaces when the surface tension is negative [67], would be expected. The DITH is also closely related to the DSCH and to the boundary-shortening model of Honda [101] because they are also based on the tensions that exist along cell-cell and cell-medium interfaces.

The DITH is very broad in its scope because it can be written in terms of surface tensions, surface energies, or the reversible work required to generate an additional unit amount of surface, since these three perspectives are equivalent to each other. Thus, effects that can be expressed naturally in terms of any one of the three can be embodied by the theory. Therefore, the DITH can be deemed to modify and subsume the other three classes of theories considered herein. In time, the influence of cell signaling [100] and other factors that affect cell affinities may also come to be understood in terms of the DITH.

The conditions necessary for each of the phenomena described in Figs. 1 and 2 can be described in terms of surface tensions and Young's equation. The basic procedure for deriving these conditions is to consider a triple junction (Fig. 7*a*) between a particular combination of cells or between cells and a medium. Figure 7*b* shows an interface between two type-*A* cells and one type-*B* cell. If the interfacial tension γ_{AA} between the type-*A* cells is sufficiently high, the triple junction will be pulled towards the left, and the type-*B* cell will be drawn between the type-*A* cells. How strong the *A*-*A* tension γ_{AA} must be compared to the *AB* tension γ_{AB} will depend on the angles formed. However, if $\gamma_{AA} > 2\gamma_{AB}$, the net force will be to the left regardless of the angles formed, and mixing is guaranteed. Thus, the relationship given between γ_{AA} and γ_{AB} is a sufficient condition for mixing. By similar arguments [13], it can be shown that if γ_{AB} is sufficiently large, $(\gamma_{AB} > (\gamma_{AA} + \gamma_{BB})/2)$, the tension along the *A*-*B* interface can push the type-*B* cell out from between the

type-*A* cells, and sorting will result. The sorting criterion is a necessary, but not sufficient, condition [13]. Similar methods can be used to determine the conditions for a wide range of cell-cell interactions (Fig. 8). When a junction between a medium and cells of one or two types is considered (Fig. 7*c*), conditions can be derived for engulfment, dissociation and a number of related phenomena (Figs. 8 and 9). The theory is also able to explain the multiple engulfment orderings [61] that sometimes occur.

The conditions shown in Figs. 8 to 10 are based on the net forces generated at a particular kind of triple junction. They indicate the motions that would occur at the triple junction and the resulting phenomena that would occur if no additional constraints were present. In a real aggregate, however, many additional constraints are present, including those that

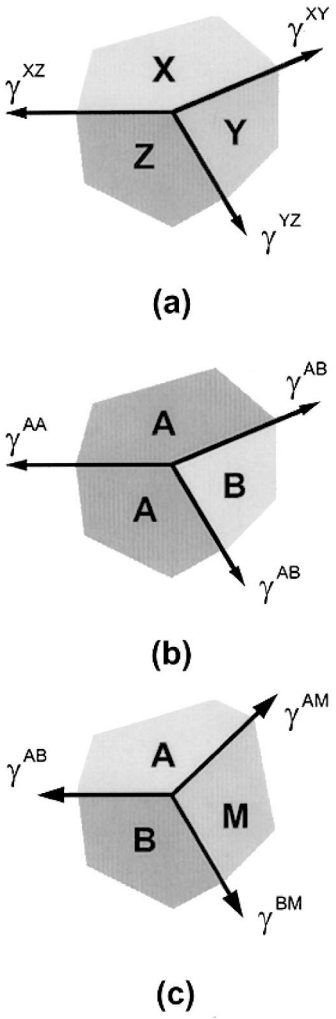

Fig. 7 Mechanics of a triple junction: *a*) A generic triple junction, a surface tension γ arises along each interface, and superscripts are used to identify the constituents of the interface; *b*) A triple junction between two types of cells. Depending on the relative strengths of the interfacial tensions, the junction may move. Movement to the left would produce mixing of the cell types, while movement to the right would produce sorting. *c*) An interface between two cell types and the medium. As noted in the text, a number of different outcomes are possible, depending on the relative values of the three interfacial tensions.

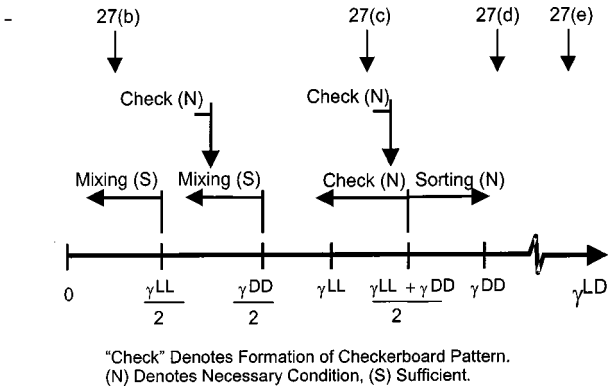

Fig. 8 Possible outcomes at a triple junction between two cell types: When two cell types interact at a triple junction, the value of γ^{LD} relative to γ^{LL} and γ^{DD} determines whether the cells will mix, sort, or form a checkerboard pattern. The value of γ^{DD} is assumed to be larger than γ^{LL}. The arrows along the top of the figure indicate where the simulations shown in Fig. 27 fall along the γ^{LD} continuum. Reprinted from [13].

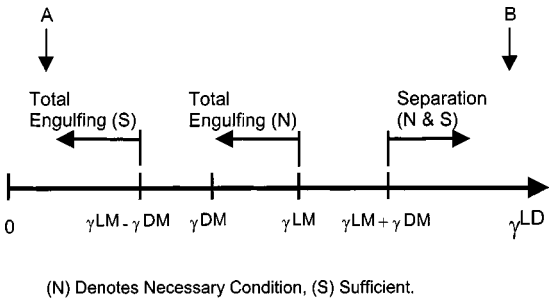

Fig. 9 Possible outcomes at a triple junction between two cell types and the medium: When two cell types and the medium interact at a triple junction, the value of γ^{LD} relative to γ^{LM} and γ^{DM} determines whether the cells will totally engulf each other, separate or, if neither of these, partially engulf each other. In this figure, γ^{DM} is assumed to be smaller than γ^{LM}, and as a result, type D cells would tend to engulf those of type *L*. The arrow labeled *A* indicates the value of γ^{LD} in the simulation reported in Fig. 29, a simulation that produces total engulfment, as predicted by the theory. Arrow *B* corresponds to an unpublished simulation that produced separation of the two tissue masses.

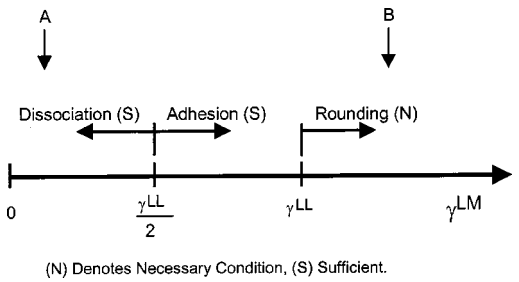

Fig. 10 Possible outcomes at a triple junction between one cell type and the medium: When one cell type interacts with the medium at a triple junction, the value of γ^{LM} relative to γ^{LL} determines whether the cells dissociate, adhere to each other or round up. Arrows *A* and *B* correspond to unpublished simulations that confirm the predictions of the theory.

arise from the fixed volume of each cell. The theory, therefore, is not sufficient by itself to prove that the reported phenomena will actually occur. The theory is also insufficient to address such important issues as the number of contiguous masses of each cell type that would be produced and whether this number would depend on the relative proportion of each cell type. To address these important questions, it is necessary to follow the detailed sequence of triple junction motions and any cell shape changes and motions that they produce. Computational models, discussed later in this review, provide an ideal means of performing these investigations.

The DITH and DAH predict different outcomes under a variety of circumstances. For example, if cells of types *A* and *B* have identical properties, in which case $\gamma_{AA}=\gamma_{BB}$, the DITH predicts sorting provided that $\gamma_{AB}>\gamma_{AA}$, while the DAH predicts no sorting. Alternatively, if two types of cells have different strengths of adhesion F^{adh} but identical interfacial tensions, the DAH predicts sorting while the DITH does not. Results from computer simulations are consistent with the DITH but not with the DAH. However, a final determination of which hypothesis is correct may require that the confusion between interfacial tension and cell-cell adhesion be eliminated and that additional experiments be carried out to measure all of the relevant cell properties.

3 CELL-CELL INTERACTIONS

3.1 Role of the observer

In all of the phenomena considered in this paper, cells undergo motions relative to each other within an aggregate. Hundreds or thousands of cells are typically involved, and the trajectories of individual cells may be quite complex [50,52]. As a result, descriptions tend to be based on the initial and terminal states of the cell mass as described by an observer and on the process by which they change from one state to another (Figs. 1 and 2). The observer must typically interpret these arrangements visually, by consciously or subconsciously comparing them with known geometric patterns. Thus, common descriptions include mixed, sorted, checkerboard pattern, and engulfed. In all cases, the visual interpretation of the observer plays a key role in the classification of the state of the aggregate. Although a number of quantitative descriptors have been introduced [27,50,73,92,102–105], many of them serve largely for comparing configurations that have been pre-classified by an observer.

The apparent subjectivity of the observer raises two questions: ''Are the patterns that observers recognize meaningful in terms of development?'' and ''Are some developmentally meaningful patterns not recognized by observers?'' The answers to both questions may be affirmative, since the catalogue of reported cell geometries [23,24,26,45,106–110], many of recognized functional importance, continues to grow.

Real cell aggregates tend to be less regularly ordered than typical classifications (Figs. 1 and 2) might suggest. Thus, sorted aggregates typically contain discontinuous phases of like cells, and checkerboard patterns typically contain a relatively high density of imperfections [13,23,25,27,83,109]. These factors must be taken into account when experimental findings are discussed, and when computational models are compared with those findings. This inherent irregularity also explains why a particular set of experimental conditions or a particular set of computer simulation parameters may illustrate a particular classification with variable success, depending on the precise initial configuration used. Consideration should be given not only to the geometry of the final configuration but also the time evolution by which it arises. A number of measures can be used for the latter, including the rates of cell diffusion and the kinetics of the growth of clusters.

3.2 Homotypic aggregates

The first group of cell-cell interactions considered are those that involve a single type of cell. These interactions include aggregation and rounding of a cell mass, and dissociation of cells from a mass (Fig. 1). Analogies exist between these phenomena and the behavior of miscible and immiscible liquids [67].

3.2.1 Self-rounding of tissue fragments

When cells in suspension contact each other, they often adhere to each other, ultimately forming a densely packed, spherical aggregate (Fig. 11) like that typically formed by an extirpated tissue fragment [12,24,111].

It has long been understood that aggregation and rounding are governed by cell surface properties [23,24,26]. Specifically, cells adhere to one another because it is energetically

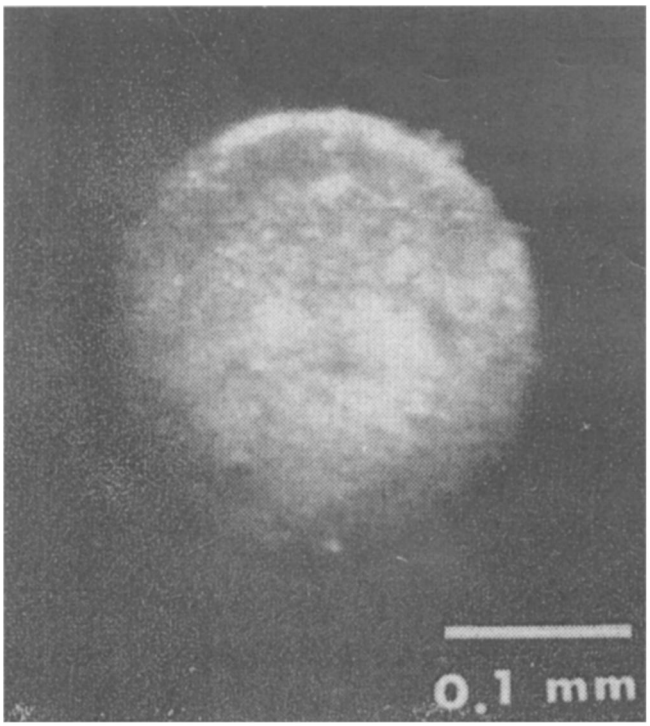

Fig. 11 Spherical mass of cells: A jagged fragment of liver cells was isolated from five-day-old chick embryos. After two days in liquid medium at 37°C, they formed the spherical mass shown. Reprinted from [12] with permission of the American Association for the Advancement of Science.

preferable for them to form a cell-cell interface rather than a cell-medium interface. This situation will occur if the reversible work of adhesion is positive. From a thermodynamic perspective, this condition explains cell-cell adhesion and the formation of dense masses in which the medium has been pushed out.

That a positive reversible work of adhesion might be sufficient to explain the rounding of the resulting dense masses or aggregates is more difficult to prove. It is not difficult to show that whenever a rearrangement occurs in a regular 2D or 3D array (as in Section 4.2 and 4.5) and the amount of cell-cell interface changes in one direction, the amount of cell-medium interface changes in the opposite direction by twice as much. This relationship occurs because the total amount of interface with cells remains constant.

Unpublished computer simulations that use the 2D cell meshes of Ref. [83] show that the rounding of an initially oblate cell mass does not produce twice as much decrease in cell-medium interface as the increase in cell-cell interface. These changes in cell areas evidently occur because the shapes of the cells inside the mass, which can change significantly during rounding of the mass [112,113], affect the amount of cell-cell interface [114]. Thus, it is difficult to argue that a negative value of W_A is sufficient to explain rounding. Rounding of a liquid droplet is somewhat different since, in the absence of any internal boundaries, it is driven solely by the surface tension that acts along the perimeter of the droplet.

3.2.2 Dissociation

Another phenomenon that has been known for many years is the ability of cells to dissociate from a mass. Dissociation can be initiated by increasing the pH of the medium [30], by adding trypsin to the medium [31], and by other means [115]. In this case, it is energetically preferable for cell boundaries to be in contact with the medium rather than with another cell. This situation is exactly the opposite of that for cell aggregation. During dissociation, the medium advances between pairs of cells, and approximately twice as much cell-medium interface is formed as the amount of cell-cell interface that is lost. Thus, the reversible work of adhesion would be expected to provide a good test for this condition, with more negative values of $W_A = W_{AA} - 2W_{AM}$ indicating a stronger tendency towards dissociation. The condition for cell dissociation corresponds to the condition for one fluid to be miscible in the other. In the latter case, the surface tension of the fluid-fluid interface becomes negative, the boundary between the fluids becomes convoluted as it increases in area, and the fluids spontaneously mix with each other [67].

Although the reversible work of adhesion W_A provides a straightforward criterion for cell aggregation and dissociation, there are several reasons why surface energy densities such as W_{AB} may be preferable for describing more complex cell-cell interactions. One of these reasons is that the use of surface energies eliminates the need to choose a reference state against which to compare a particular boundary type [27]. This advantage is particularly relevant in the description of systems that involve multiple cell types. Surface tensions also lend themselves to the construction of free body diagrams for the investigation of force interactions at triple junctions between cells and to the use of Young's equation. In addition, surface tension is a quantity that can be measured [84,85,90,113,116,117]. A final reason to use surface (interfacial) tensions is that the most recent understanding of cell-cell interactions [13,46,82] is expressed in those terms.

3.3 Interactions between tissue fragments

When more than one cell type is present, many kinds of cell-cell interactions are possible (Fig. 2). This section deals with those interactions in which all cells of each kind are grouped into a single contiguous mass or tissue fragment. Sorting and other phenomena where topological changes occur, such as the merging of groups of cells of like kind, are discussed in Section 3.4. All of the interactions considered in this section have direct analogs with immiscible fluids [118,119].

3.3.1 Partial or total engulfment

When tissue fragments of two different histological types are brought into contact with each other, the cells from one may spread over and partially (Fig. 12) or totally engulf those of the other [12,23,26,32,35,85,113,120]. Many combinations of tissues have been studied, as shown in Table 1 of Ref. [23].

The order of engulfment is hierarchical in the sense that if tissue *A* engulfs tissue *B*, and *B* engulfs *C*, then *A* will also engulf *C* [12,23,24]. Phillips and Davis [113] advanced the concept that the process of engulfment was governed by surface tensions. This hypothesis has now been verified through an extensive set of experiments by Foty *et al* [85], who showed that tissues having lower surface tension normally

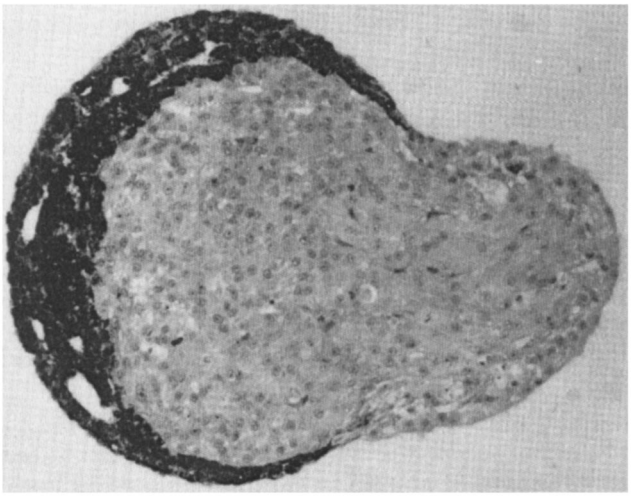

Fig. 12 Partial tissue engulfment: Pigmented retinal tissue (darkly pigmented cells) and heart tissue (unpigmented cells) from ten-day-old chick embryos were brought into contact with each other. After being kept in organ culture conditions for two days, the retinal tissue partially engulfed the heart tissue. Reprinted from [26] with permission of CRC Press.

engulf those having higher surface tensions [85] according to the same pattern that governs immiscible fluids [118,119].

3.3.2 Separation of homotypic masses

When droplets of certain combinations of immiscible fluids are brought together, they remain separate from each other [118,119]. An analogous phenomenon, tissue segregation, has been reported in cardiac tissues, sponges and hydra [29,121–123].

3.4 Interactions between cells in heterotypic aggregates

Two or more types of cells can be mixed to form a heterotypic aggregate and can be used as an initial configuration for experiments of cell-cell interactions. A broad range of cell-cell interactions is then possible (Fig. 2). The most important of these interactions is spontaneous sorting of the cells by type. For the sake of completeness, two other phenomena that involve multiple cell types are included here: spontaneous mixing of cells and the formation of regular patterns in epithelia. For this purpose, epithelia are viewed as a specialized type of 2D aggregate.

3.4.1 Sorting

The ability of cells of different types to sort out spontaneously from each other has been known since the 1950s [30,31,86,88,124]. Beginning in the 1960s, an intensive program to elucidate the mechanism by which this intriguing phenomenon occurs was led by Steinberg and others [11,12,23–25,32–35,40,42,61,64–66,84,85,89–92,112,113,116,125–129]. Since this quest has been chronicled elsewhere [23,24,26], it is not repeated here.

A concise summary of sorting has been provided by Armstrong [26]:

> (1) sorting is the process by which cohering, disorganized cell populations establish homogeneous tissues; (2) cell sorting can occur with mixed cell populations whether the cells are from tissues that normally are in contact or are from tissues that *in situ* are not associated; (3) the patterned array generated by cell sorting usually is reproducible for a given pairing of cell types; and (4) if the cell types combined in a sorting experiment in organ culture are from tissues normally in association *in vivo*, then the final organization frequently bears a striking similarity to the organization of those two tissues *in vivo* (Table 1 of Ref. [26]).

Figure 13 shows a series of images that are representative of the process of sorting. When a heterotypic mass is first constructed (Fig. 13*a*), its cells are highly disordered and the mass has an irregular perimeter. With time (Fig. 13*b*), groups of like cells become associated, producing islands of increasing size within the aggregate. The outer border becomes increasingly smooth with time and consists of cells that are predominantly of a single type. Eventually (Fig. 13*c*), the mass reaches a configuration in which further bulk changes are not apparent. In this state, cells of one type typically engulf one or more large islands of cells of the other type, and the perimeter of the mass is smooth, but not necessarily spherical. A single sphere of one cell type completely sur-

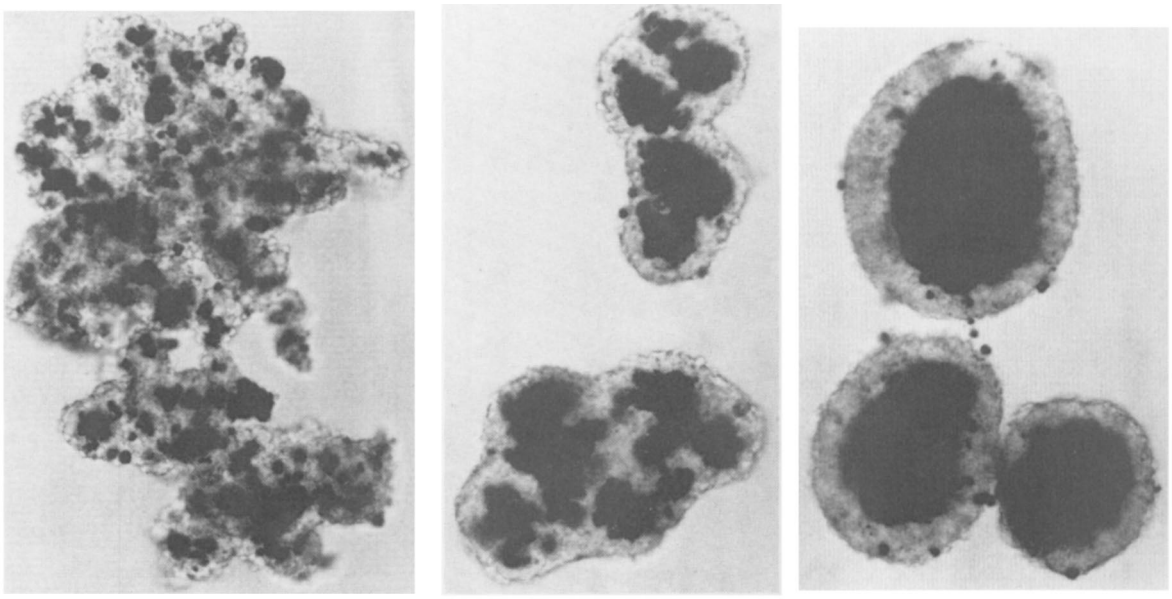

(*a*) (*b*) (*c*)

Fig. 13 Cell sorting: Pigmented retinal tissue (darkly pigmented cells) and neural retina (unpigmented cells) from seven-day-old chick embryos were maintained in stirred suspension culture. *a*) After five hours, the cells are highly disordered, and the perimeter of the aggregate is convoluted. *b*) After 19 hours, the pigmented retinal cells have left the surface of the aggregate and have formed homotypic clumps, and the surface of the aggregate has become smooth. *c*) By two days, the clumps and the mass as a whole have become substantially rounded. Reprinted from [26] with permission of CRC Press.

rounded by a sphere of another type [12,113], the state that theoretically has the lowest system energy, is seldom observed.

Many combinations of tissues have been investigated by means of this method (Table 1 of Ref. [23]), and the role of factors such as the proportions of each cell type present [24] have been studied using both 2D [50,126–128] and 3D aggregates [23,24,26]. Other studies have examined the roles of specific cytoskeletal components [35], cell surface proteins [42,64–66,127], and fibronectin [61], as well as the effect cell position within a limb has on sorting [104] and the effect of culturing cells with and without glucose [63]. Some understanding of the cell-level aspects of the sorting process has also been gained [127].

Many key features of cell sorting have now been established. The motions of individual cells involve local, cell-level deformations [127] and produce motions of cells that are like those of a random walk [50,52,130]. These motions cause individual cells and groups of cells of like kind to contact each other and to form chains or bridges between them [24]. Over time, the accretion of clumps of like kind causes the mean size of the resulting islands to grow [24,92,103]. This process typically produces one or more large islands but may produce many small clumps or thin chains, especially in 2D systems [24,126].

Along the perimeter of the mass, the cells tend to interact according to the principles of tissue engulfment. Thus, the islands tend to be formed from the cell type that would be engulfed when tissue fragments of the same kinds are brought into contact with each other. Engulfment of edge cells often occurs much more quickly than does sorting [12,24,26]. The final, sorted configuration produced from mixed cells is the same as that produced when tissues of those same cell types are brought into contact [12,23,26,32,92,131]. Thus, as shown in Fig. 2, whether two kinds of cells start as two homotypic tissue fragments or as a thoroughly mixed heterotypic mass, they typically produce similar final configurations, in which the cells are sorted and the cells with the highest surface tensions are engulfed [12,26].

The final outcome of the sorting process is not always this straightforward because the degree of sorting depends strongly on several factors, including the types of cells used, the amplitude of the membrane cell fluctuations, the aggregate size, and the volume fraction of each cell type. In addition, it is possible for an outer rim and internal islands to be formed of the same cell type [35] and for the final engulfment order to change [61]. Computational models, which are discussed in detail in Section 4, shed light on several of these features of sorting.

3.4.2 Mixing

In sorting, the common boundary between dissimilar cells is minimized. If it were energetically preferred for these boundaries to increase, dissimilar cells would spontaneously mix. Sorting and mixing (intercellular invasion) and the biological conditions under which transitions from one behavior to the other occur have been investigated [102]. In fluids, spontaneous mixing of miscible fluids is well known [67]. Although fluids can protrude and interdigitate with each other at scales as fine as molecules, tissue intermingling is limited by cell size and internal structure. The protrusions of cells into surrounding medium shown in Fig. 7 of Ref. [101] may be a related phenomenon.

3.4.3 Checkerboard patterns

A number of stable patterns of intermixed cell types have been identified in epithelia [45,106,108,109]. That these patterns remain stable suggests that either the cells are tightly bound or that for some other reason it is energetically beneficial for them to remain in that configuration. In the case of checkerboard patterns (Fig. 14), the amount of both types of homotypic boundary is minimized [27,83]. This requirement is slightly different from that of mixing, where only one type of homotypic boundary need be minimized. Thus, like the other final configurations shown in Figs. 1 and 2, checkerboard patterns can be explained in terms of cell-surface properties.

4 COMPUTATIONAL MODELS OF CELL-CELL INTERACTIONS

Computational models provide an indispensable complement to experimental and theoretical studies. General reasons for this distinctive role are presented in the Introduction to this paper and elsewhere [18]. The brief survey of experimental and theoretical approaches included in this work showed that these approaches raise a number of issues that they cannot address conclusively. As this section will show, computational models have been able to address many of these issues and thereby provide critical insights into the mechanics of cell-cell interactions. Many of the computational studies named in this review are rich in analysis and insight, and much can be learned from reading the original works. The

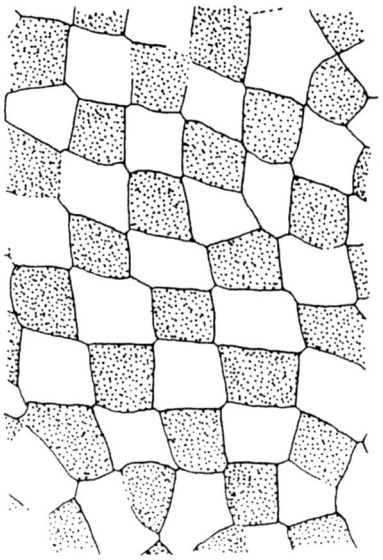

Fig. 14 Checkerboard pattern: A tracing of the luminal surface of a mature quail oviduct epithelium showing the arrangement of the *C*-cells (shown stippled) and the *G*-cells. Reprinted from [45] with permission of the Company of Biologists Ltd.

purpose of this review is to highlight some of their main contributions and to show how they relate to each other.

4.1 A common framework

All of the computational models considered here are founded on the concept that cell-cell interactions produce a sequence of local changes. These local changes range in scale from the exchange of entire neighboring cells to arbitrarily small incremental displacements at triple junctions. The configuration space in which these changes occur is assumed to be smooth, and any anomalies in the system free energy that result from the discrete nature of a particular model are explained through the use of thermodynamic concepts [27].

The driving force behind all of the models is an assumed property of the cell-cell or cell-medium interface. This property may be expressed either in terms of energy per unit of interface or as a surface tension, although these representations are equivalent to each other [27,67,82,84]. The value of this property depends on the histological type of the cell or cells that participate in the interface. In all cases, the model finds a configuration that minimizes a weighted sum of the boundary lengths, where the weighting factors are the values of the assumed interface property, subject to certain constraints related to cell volume and cells remaining contiguous. If the model is framed in terms of energy, the resulting state corresponds to a local system free energy minimum. If framed in terms of forces, it is an equilibrium configuration. The models do not necessarily find the configuration of lowest free energy, just as real aggregates of cells do not. Cell motions are driven by differences in this property from one interface type to another.

For many years, this cell property was understood to be the strength of the cell-cell adhesion along that interface. Although early analysis [37,116] identified adhesion and surface tension as possibilities, partiality to adhesion and the subsequent process by which this explanation became a paradigm led most authors to assume that the governing property was adhesion. Recent work has clarified the differences between adhesion and interfacial tension, and has shown that the latter is the critical property [13,46,82,85]. In all the models except the finite element model, the interfacial property is reported as arising from adhesion. These papers are best understood as having ascribed to adhesion a boundary type-specific energy density that actually arises from surface tension. If the values of this energy density are interpreted as arising from surface tension instead, and the wordings of the explanations correspondingly changed, the basic findings of all of the models can be harmonized. A similar reinterpretation is required of much of the experimental literature [13,82].

To present the computational models and their findings, a series of tables are used. These tables make it possible to compare the methods used (Table 2), the contributions made by various researchers using each of these methods (Table 3) and the conditions found for various cell-cell interactions (Tables 4 and 5).

4.2 Cell-lattice models

These clever methods were developed at a time when it was often difficult to obtain access to computers and when memory and computational capabilities were very limited. The insights provided by early cell-lattice models (Table 2) are remarkable given the facilities and computing languages available at the time. Many researchers used this method and made important contributions (Table 3).

The first computational models of cell-cell interactions were based on regular, square [40,41,131,132,136] or hexagonal [130,137] lattices, in which each lattice site represents a cell. A number of these papers are reprinted in Mostow [138]. In a square lattice model (Fig. 15), each cell is considered to be in contact with its four neighbors, while in a hexagonal array, each cell contacts its six neighbors.

The basic steps in a lattice-based model are the following [41]:

1) A routine is used to randomly assign types to each of the lattice sites [41]. Alternatively, a non-random initial pattern may be set by hand [40,41].
2) Cells are then chosen at random, with [130] or without controls, to ensure that each cell is considered an equal number of times.
3) For each randomly chosen cell, one of its neighbors is randomly chosen.
4) The possibility of exchanging these two cells (Fig. 15) is then considered. Based on various rules that consider nearest neighbors [41] or more distant neighbors [131,132], a measure of the change in the free energy of the system is calculated.
5) Based on this change in energy, a decision is made whether or not to exchange the pair of cells under consideration. In some versions of this approach, exchanges may be made even if the system free energy is not thereby decreased. Some implementations use a probability function as part of the decision-making process [133], while most simply use threshold values.
6) Steps (2) through (5) are repeated a specified number of times or until some other criterion is satisfied. A pseudotime is often defined based on the ratio of the number of cycles of steps (2) through (5) to the number of cells in the original array.

The cell-lattice model is relatively straightforward to program, it runs quickly on a computer, and it can simulate a wide range of cell-cell interactions. Figure 16 shows initial, intermediate and final configurations of a typical simulation of cell sorting.

Collectively, simulations based on cell-lattice models made a dramatic impact on the cell-cell interaction literature. They showed that differences in the properties of cell interfaces could drive a wide range of phenomena and led to quantitative statements of the conditions needed for many of them (Table 4). These models provided a means of investigating important mathematical issues related to path, uniqueness and stability. They also made it possible to identify parameters that could describe the time course of various phenomena [41,105,130,133,139].

Table 2. Comparison of different types of computational models: The table is not exhaustive

Approach	How a New Configuration is Produced	Increment	Advantages	Disadvantages
Cell Lattice	Cell pair exchange	Complete cells are exchanged	Straightforward to program	Real cells cannot simply exchange with each other
		Six full interfaces may be affected	Runs quickly on a computer	Many full edges are altered with each exchange
			Simulates a wide range of phenomena	
Sub-cellular Lattice	Type re-assignment of lattice sites at the edge of a cell	Cell edge moved by a discrete increment	Straightforward to program	Cell boundaries are forced to follow lattice boundaries; thus realistic, angled boundaries are not possible
			Runs quickly on a computer	
			Simulates a wide range of phenomena	
Centric Models	Forming point is moved	All immediately surrounding cells are also forced to reshape	Allows cell edge lengths to change smoothly	Volume of individual cells may not be conserved
		Displacement increment is arbitrary		Only suitable for cells of isotropic shape
Boundary Vertex	Coordinated movement of a pair of nodes	Four cells are reshaped	Allows cell edge lengths to change smoothly	Does not model cytoplasm viscosity
		Displacement increment is arbitrary	Gives meaningful angles at triple junctions	
			Cell volume is conserved	
Finite Element	Imbalanced forces are calculated at the beginning of each time step, and are used to drive simultaneous incremental deformation of all of the cells	Each node can move independently (subject to volume constraints)	Allows cell edge lengths to change smoothly	Programming large-deformation FE code to model cells is quite challenging
		Displacement increment is arbitrary	Gives meaningful angles at triple junctions	Commercial FE codes are not suitable
			Cell volume is conserved	Requires the most computing power of all of the methods reviewed
			Effect of cytoplasm viscosity is modeled accurately	Difficult to extend to 3D
			This is the only approach to give an accurate time scale	
			Arbitrary (anisotropic) cell shapes can be modeled	

That the cell-lattice model is so effective in modeling real cell aggregates is somewhat surprising since the concept of cell exchange on which the model is based is not a known behavior of cells. Also, since the minimum difference between two configurations requires the exchange of two complete cells, the sequence of states through which the aggregate passes is relatively coarse. Taking such large steps may give access to aggregate configurations that would not occur naturally. That large steps could be an issue is apparent if, rather than exchanging adjacent cells, one were to exaggerate the situation and allow non-adjacent cells to be exchanged. This issue notwithstanding, the ease with which lattice models can be programmed and the extent of their success in modeling cell-cell interactions explains why they continue to be used [105,133].

4.3 Centric models

The next family of models employs a cell-centric approach (Fig. 17), which uses Dirichlet or Voronoi tessellation [140] of the plane. Honda [43,101] showed that a Voronoi tessellation provides a close geometric approximation of the cell boundaries in a number of 2D aggregates. In a tessellation of

Table 3. Contributions of individual modeling studies: The table is not exhaustive

Model Type and Name	Cell Geometry	Range of Interaction	Principle of Operation	Authors and Date	Principal Contribution(s)
Cell-Lattice Models					
Cell Lattice	Square	Two cells	Cell-pair exchange	Goel *et al* [41]	Apparently, the first computer simulation of cell-cell interactions. Addressed the important mathematical issues of path and stability. Identified many conditions, including those for checkerboard pattern, partial and total engulfment and separation. Represented the relationships between these conditions using a clever fold-up polyhedron model Considered 2 and 3 cell types Some 3D simulations.
—	Hexagonal	One cell	—	Antonelli *et al* [130]	First use of hexagonal grid Introduced concept of metabolic energy Allows cell exchanges for which the change in system energy is neutral Argues for eccentric rather than concentric total engulfment Considered different proportions of cell types Identified some mathematical errors in previous works
—	Square	One cell, but more in homotypic clump	—	Gordon *et al* [40]	Highlights the high apparent viscosity of cell aggregates In-depth discussion of relevant experiments by others, including experiments in which aggregated clumps are subsequently pulled apart
—	—	One to five cells	Multiple-cell exchange	Goel and Rogers [131]	Investigated a wide range of phenomena
—	—	One to five cells	—	Rogers and Goel [132]	Considered different ratios of each cell type Investigated the effect of changes to the interaction range
—	—	One cell	Cell-pair exchange	Mochizuki *et al* [133]	Introduced measure $q_{B/B}$ of black neighbors to black cells, and isolated black cell parameter IBC Considered several probability distributions for the exchange rule
—	—	—	—	Mochizuki *et al* [105]	Compared lattice simulations with experiments and estimated properties of real cells
Centric Models in Which a Cell is Defined by a "Central" Point					
Cell aggregate	Dirichlet	One cell	Geometric description	Honda [43,101]	Showed that cell shapes are similar to Dirichlet (Voronoi) tesselations Extensive investigation of cell geometry, and comparison with other physical systems such as bubble rafts
Dirichlet with rectang-ular boundary	Dirichlet	Surrounding cells	Dirichlet forming point is moved to reduce aggregate free energy	Sulsky *et al* [44]	Detailed review of previous models Used area constraint on cells First use of cell viscosity
Dirichlet with maximum cell radius	Dirichlet	Surrounding cells	Forming point is moved	Granger and Sawada [134]	Modeled a wide range of phenomena Identified conditions for each phenomena
Boundary Vertex					
Boundary Shortening	Polygons	The cells at each triple junction	Pairs of nodes are displaced	Honda [101]	First representation of cells as polygonal areas First description of local conformational change (edge flip) associated with cell rearrangement Introduced boundary shortening concept Introduced ratios of total boundary length in aggregate to that following boundary shortening
Weighted Boundary Shortening	—	—	—	Honda *et al* [45]	

Table 3. (Continued)

Model Type and Name	Cell Geometry	Range of Interaction	Principle of Operation	Authors and Date	Principal Contribution(s)
Finite Element Models					
Sub-cellular Lattice Models					
Lattice-defined Boundary	Irregular, consisting of a contiguous set of square sub-cellular lattice sites	One sub-cellular lattice site	Sub-cellular lattice sites are reassigned to the type of the adjacent cell	Graner and Glazier [135]	First use of High-Q Potts model to study biological cells Modeled cell sorting
—	—	—	—	Glazier and Graner [27]	Modeled a wide range of phenomena Used a large number of cells (eg. N+100) Identified a conditions for each phenomena
Finite Element	Polygons	The cells at each triple junction	Nodes are moved simultaneously	Brodland and Chen [83]	First use of finite element formulation to model cell-cell interactions Introduced concept that cell sorting and tissue engulfment are driven by differences in interfacial tensions Modeled a number of phenomena Challenge to Differential Adhesion Hypothesis (DAH)
—	—	—	—	Brodland and Chen [82]	Resolved concept of differential interfacial tension driven motions with experimental literature on tissue engulfment Identified conditions for Engulfment phenomena
—	—	—	—	Brodland [13]	Formalized statement of Differential Interfacial Tension Hypothesis (DITH) Resolved the DITH with computer simulation literature Comprehensive set of conditions for wide range of phenomena Investigated interactions between 3 and 4 cell types Showed that the conditions on pairs of cell types continue to apply

Table 4. Conditions for interactions between cells: As noted in the text, additional conditions must be satisfied for some of these phenomena.

Phenomenon	Brodland, 2002 [13]	Brodland and Chen, 2000 [83]	Graner and Sawada, 1993 [134]	Honda *et al*,, 1986 [45] (1)
Sorting of L and D	$\gamma^{LD} > \frac{\gamma^{LL}+\gamma^{DD}}{2}(N)$	$\gamma^{LD} > \frac{\gamma^{LL}+\gamma^{DD}}{2}(N)$	$e^{LD} > \frac{e^{LL}+e^{DD}}{2}$ $e^{LL}+(e^{DM}-e^{LM}) > e^{LD}$	
Mixing of L and D	$\gamma^{LD} < \frac{\gamma^{LL}}{2}(S)$ $\gamma^{LD} < \frac{\gamma^{DD}}{2}(S)$	$\gamma^{LD} < \frac{\gamma^{LL}}{2}(S)$ $\gamma^{LD} < \frac{\gamma^{DD}}{2}(S)$		
Checkerboard of L and D	$\gamma^{LD} \cong \frac{1}{\sqrt{2}}\gamma^{LL}(N)$ $\gamma^{LD} \cong \frac{1}{\sqrt{2}}\gamma^{DD}(N)$	$\gamma^{LD} < \gamma^{LL}(N)$ $\gamma^{LD} < \gamma^{DD}(N)$	$e^{LD} < \frac{e^{DD}+e^{LL}}{2} < 0$	$J^{LD} \cong 2J^{DD} - J^{LL}$

(1) Algebraically re-arranged

this kind, the mesh is completely defined by the locations of so-called forming points, and each point in the plane is assigned to the forming point to which it is closest. The boundaries that arise between these regions are perpendicular bisectors to lines joining pairs of forming points. When the division process is complete, one polygonal domain or cell surrounds each forming point.

If a single forming point is moved (Fig. 17), the geometries of the cell associated with it and of the immediately adjacent cells are altered. This action changes the lengths of a number of the cell-cell boundaries and may even change the conformation of the sheet. The geometric changes that result from displacements of the forming points provide the basis for the cell-centric model.

This cell-centric model uses the following algorithm:

1) Forming points are distributed over the domain of interest. The number of cells will equal the number of forming points, and regulating the relative spacing of the forming points [141] can control the range of the cell size distribution. If desired, the forming points near the edge of the

Table 5. Conditions for interactions between cells and medium: As noted in the text, additional conditions must be satisfied for some of these phenomena.

Phenomenon	Brodland, 2002 [13]	Brodland and Chen, 2000 [82]	Graner and Sawada, 1993 [134]	Foty and Steinberg, 1995 [84] (1)
Total Engulfment of L by D	$\gamma^{LD}<\gamma^{LM}(N)$ $\gamma^{LD}<\gamma^{LM}-\gamma^{DM}(S)$	$\gamma^{LD}<\gamma^{LM}-\gamma^{DM}(S)$	$e^{LD}<e^{DD}+(e^{LM}-e^{DM})$ $\frac{e^{DD}+e^{LL}}{2}<e^{LD}$	$\gamma^{LD}<\gamma^{LM}-\gamma^{DM}$
Partial Engulfment of L by D	This occurs when neither Total Engulfment nor Separation occur	$\gamma^{DM}-\gamma^{LM}<\gamma^{LD}<\gamma^{LM}+\gamma^{DM}(N)$ $\gamma^{LM}<\gamma^{LD}<\gamma^{DM}(S)$		$\gamma^{LM}-\gamma^{DM}<\gamma^{LD}<\gamma^{LM}+\gamma^{DM}$
Separation of L and D	$\gamma^{LD}>\gamma^{LM}+\gamma^{DM}$	$\gamma^{LD}>\gamma^{LM}(N)$	$e^{LD}>e^{LM}+e^{DM}$	$\gamma^{LD}>\gamma^{LM}+\gamma^{DM}$
Dissociation	$(N\&S)$ $\gamma^{LL}>2\gamma^{LM}(S)$	$\gamma^{LD}>\gamma^{LM}+\gamma^{DM}(S)$		

(1) Converted from reversible work of adhesion to surface tension as defined herein.

domain can be reflected about the edge of the patch in order to induce the formation of a straight edge there [141]. If this procedure or some other size-limiting constraint [134] is not applied, some of the edge cells will extend outwards without bound.

2) A Dirichlet (or Voronoi) tessellation is constructed from the forming points. Although each resulting region is normally understood to be a single cell, it can be interpreted as a cluster of like cells [44].
3) For each time step, a complex series of calculations is used to determine the incremental forming point displacements that provide the steepest descent along the free energy surface and that just balance this decrease with the energy dissipation caused by the cell viscosity μ. These displacements are driven by energy changes produced by changes in the lengths of the cell-cell boundaries and are constrained by side conditions that maintain the volume of individual cells.
4) Steps 2 and 3 are repeated until a final configuration is reached or until a temporal condition is satisfied.

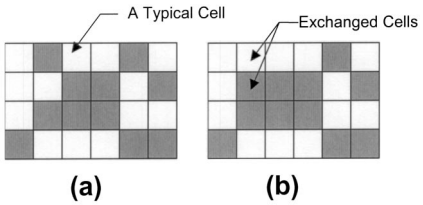

Fig. 15 Cell exchange model: In this model, each biological cell occupies one cell of the grid. Square or hexagonal grids can be used. Here, light cells represent one cell type while dark cells represent another. The basic algorithm involves the exchange of entire cells, as has happened between parts *a* and *b* of the figure.

A cell-centric model has two main advantages over a cell-lattice model: cells take the shape of polygons rather than being restricted to fixed, uniformly sized lattice shapes, and the cell geometries can change smoothly over time rather than having to take discrete, cell exchange-sized steps. In order to consider cases where cells do not form a confluent sheet, Graner and Sawada [134] enhanced the cell-centric model by allowing cell boundaries to be further defined by a specified maximum radius. Simulations of checkerboard pattern formation and of sorting are shown in Figs. 18 and 19. Simulations based on this approach made it possible to investigate a wide range of additional phenomena. The conditions identified for these phenomena (Tables 4 and 5) are in close agreement with those found using cell-lattice models.

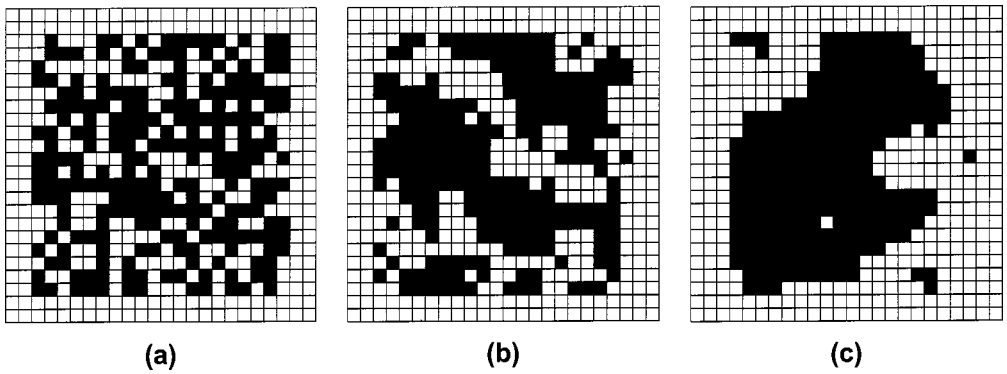

Fig. 16 Simulation of cell sorting by cell exchange: In this simulation, the original authors set the parameters such that *D-D* interfaces are preferred over *L-L* and *L-D* interfaces. The result is that the cells sort: *a*) the initial configuration; *b*) an intermediate state; *c*) the final state of the system. Sorting is nearly complete and is aided by the migration of small clumps that are an artifact of the algorithm used. The time scale was not reported in the original article. Reprinted from [40] with permission of Harcourt Inc.

The main drawback of this type of cell-centric model is that the cells cannot take on any arbitrary polygonal shape, but only those shapes permitted by a Dirichlet tessellation. Thus, cells with a strong anisotropic geometry cannot be modeled.

4.4 Boundary vertex models

An approach that allows cells to take general polygonal shapes and that removes the restrictions inherent in centric models is the boundary vertex model. In this model, polygonal cells are defined by the spatial coordinates of their vertices (Fig. 20). Two versions of this model have been reported: a boundary-shortening version, in which the objective is to minimize the total boundary length [101], and a weighted boundary-shortening model, which allows the influence of different boundaries to be given different weights in the minimization process [45].

The following is the basic approach used in this model:

1) An initial configuration is constructed by tracing the geometries of cells in actual aggregates or by some other means.
2) One cell-cell boundary is chosen at random. The nodes on this side are then moved in such a fashion that the areas of the four cells affected by their movement do not change. If node P in Fig. 20 is moved along a line parallel to AB, the area of the cell that includes points A, P and B remains unaffected. A similar result occurs when node Q is moved parallel to CD. Finally, if nodes P and Q are moved by suitable amounts in opposite directions, the areas of the cells $BPQD$ and $APQC$ remain constant. In the boundary shortening procedure, the new positions P' and Q' of nodes P and Q are chosen to minimize the total length $AP'+BP'+P'Q'+Q'C+Q'D$. In the weighted version, each side length is multiplied by a weighting factor proportional to the energy associated with its boundary type, and the weighted sum is minimized. A

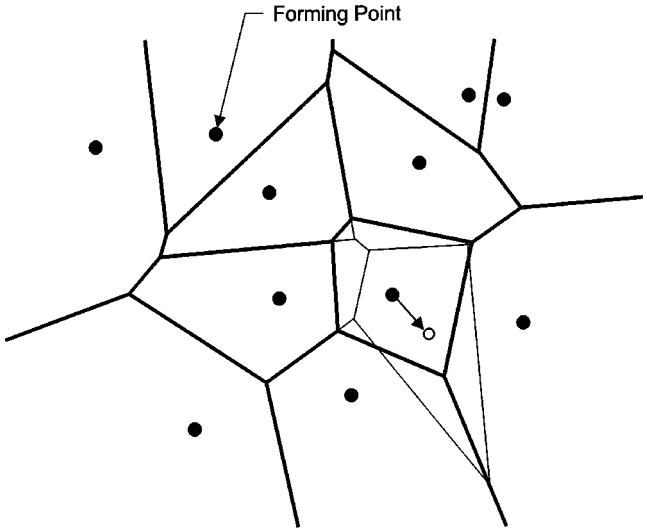

Fig. 17 Cell-centric model: In this model, the boundaries of the cells are determined by a Voronoi (or Delauney) tessellation of the plane based on the positions of the forming points. If the tessellation points are placed entirely at random, irregular cell shapes result and cell sizes vary widely. The wide lines indicate a tessellation based on the forming points shown as filled-in circles. The arrow indicates a small displacement of one of the forming points, and the narrow lines show the modified tessellation that results. The lengths of several boundaries are changed and the conformation of the mesh is altered.

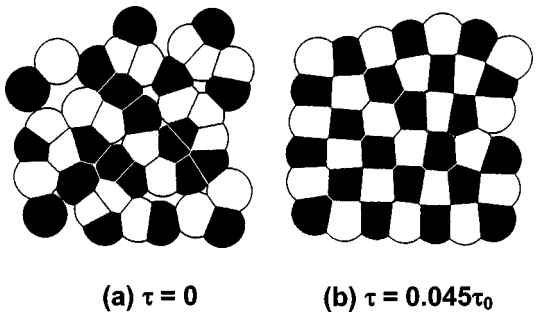

Fig. 18 Simulation of checkerboard pattern formation using a cell-centric model: When it is energetically preferable for a cell to contact a cell of a different type than to contact one of its own type, a checkerboard pattern results. In this model, the Voronoi boundaries have been augmented with circular boundaries of specified radius so that the cells need not remain contiguous with each other. Reprinted from [134] with permission of Harcourt Inc.

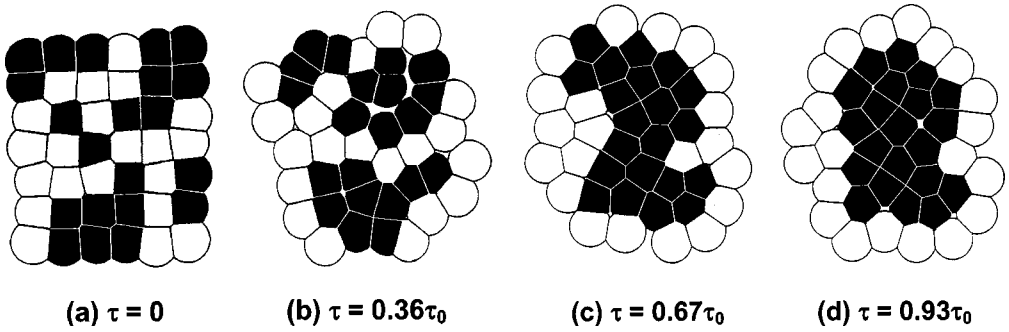

Fig. 19 Simulation of cell sorting using a cell-centric model: *a*) initial configuration; *b*) and *c*) intermediate states, and *d*) final configuration. The boundary parameters have been chosen so that it is energetically preferable for the cells to form a D-D boundary rather than an L-D boundary and to form either of these rather than an L-L boundary. The parametric values for the D-M and L-M boundaries are set equal to each other. The resulting sorting is explicitly predicted by theory, but the engulfment of the darker cells by the lighter ones is not. Reprinted from [134] with permission of Harcourt Inc.

neighbor change algorithm similar to that shown in Fig. 21 is used to accommodate cell rearrangement.

3) Step 2 is repeated until no further movement occurs.

Boundary-shortening methods in conjunction with a total boundary length parameter have been quite successful in the characterization of the geometry of cell sheets and tissue cross-sections [43,101]. The weighted version has also been effective in the modeling of a transformation that produces a checkerboard pattern [45].

The primary drawback of vertex methods is that they do not allow the mechanical effects of the cell cytoplasm to be incorporated and, as a consequence, they cannot be directly correlated with time.

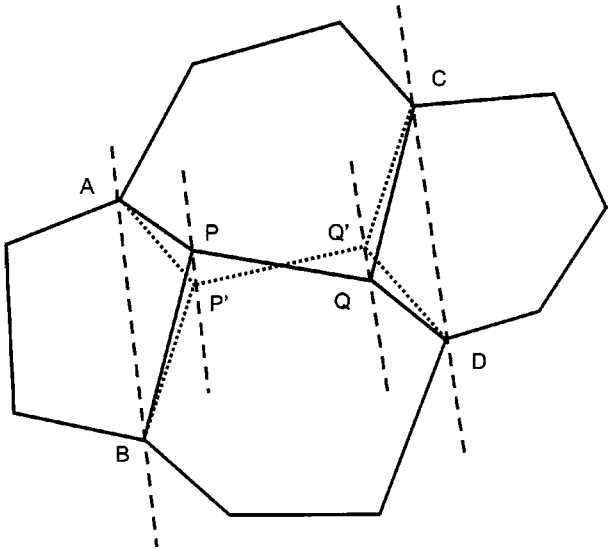

Fig. 20 Vertex Model: In this model, each cell is defined by the positions of its vertices. The algorithm moves adjacent vertices in pairs (from PQ to $P'Q'$, for example) in such a way that the areas of all of the cells are unchanged. Changes in boundary length result, and the configuration that minimizes the energy of the five affected boundaries is chosen. Reprinted from [45] with permission of the Company of Biologists Ltd.

4.5 Sub-cellular lattice models

To maintain the ease of programing and fast run times characteristic of lattice methods but reduce the size of the minimum geometric change, a series of high-Q Potts models and other, related models, were developed [27,135,142,143]. In these models, cells encompass approximately 40 contiguous sites on a square lattice (Fig. 22*a*) and a large number of cells (eg, 1000) can be modeled without difficulty. Sites along the edge of each cell are selected at random and considered for transformation to the type of the neighboring cell (Fig. 22*b*). In essence, this action moves the location of the cell boundary from one side of the lattice site to the other. This procedure allows much smaller stepwise geometric changes than the whole-cell exchanges required in cell-lattice models. In this model, a Hamiltonian H is defined, such that

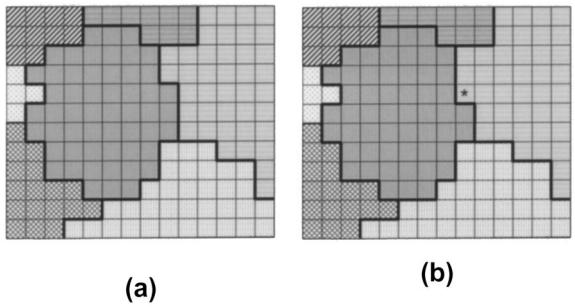

Fig. 22 Sub-cellular lattice model: *a*) In a sub-cellular lattice model, each biological cell (demarcated by shading) occupies multiple lattice cells (demarcated by the rectangular grid). Normally, the lattice sites from which a single cell is formed are simply connected. *b*) The algorithm can change the type of a lattice site to the type of an adjoining lattice site, as has happened in the case of the site marked with an asterisk. The usual consequence of this change is to modify the position of the boundary between adjacent cells.

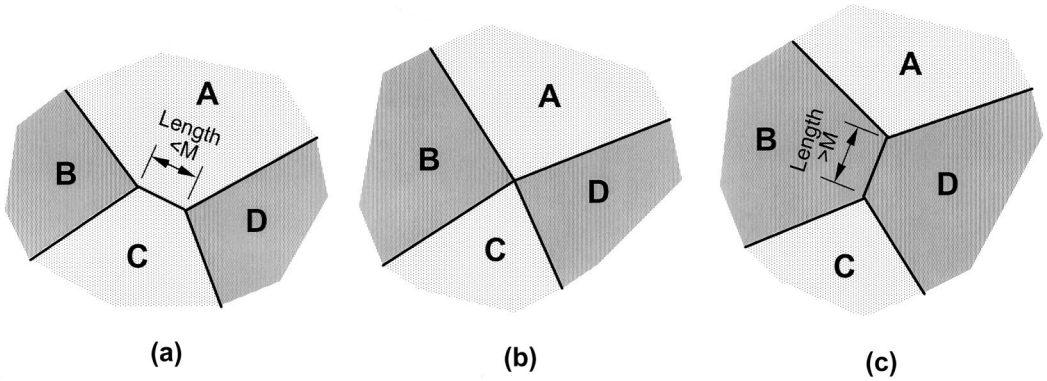

Fig. 21 Standard cell-rearrangment algorithm: *a*) Two cells A and C are initially in contact; *b*) If the length of the A-C boundary shortens sufficiently, the configuration shown will result; *c*) increasing contact between cells B and D will produce a new finite-length interface between these cells. The usual numerical implementation of the algorithm involves a direct change from a configuration in which the length of the A-C interface ceases to be longer than M to a new configuration in which the A-C interface is exchanged for a new B-D interface, which is assigned a length somewhat greater than M. A slight change in cell areas occurs, and this change may or may not be corrected during subsequent steps of the algorithm. Reprinted from [46].

$$H=\sum_{(i,j),(i',j')neighbors} J(\tau(\sigma(i,j)),\tau(\sigma(i',j')))\times(1-\delta_{\sigma(i,j),\sigma(i',j')})+\lambda\sum_{spin\ types\ \sigma}[a(\sigma)-A_{\tau(\sigma)}]^2\theta(A_{\tau(\sigma)}) \quad (7)$$

where $J(\tau,\tau')$ is the surface energy between spins of type τ and τ', λ is a Lagrange multiplier specifying the strength of the area constraint, $a(\sigma)$ is the area of cell σ, and A_τ is the target area for cells of type τ. The target area A_M of the medium is set to be negative, and $\theta(x)=\{0$ if $x<0;1$ if $x>0\}$ to suppress the area constraint on it.

The following is a typical algorithm used in a sub-cellular lattice model:

1) A starting configuration is generated. The identity of each cell is uniquely defined by its *spin* σ and its type is identified by a parameter τ. Cells need not be simply connected.
2) A lattice site (i,j) is chosen at random and with probability

$$P(\sigma(i,j)\rightarrow\sigma(i',j'))=\begin{cases}\exp\left(-\dfrac{\Delta H}{kT}\right) & \text{if } \Delta H>0\\ 1 & \text{if } \Delta H\leq 0\end{cases} \quad (8)$$

the spin of site (i,j) is changed to that of site (i',j').

3) Step 2 is repeated until meaningful exchanges cease or until another criterion is satisfied. In this process, one Monte Carlo time step (MCS) is defined to require 16 times as many iterations of step 2 as there are spins in the array.

This approach involves a number of free parameters that must be pre-assigned. One of these parameters, λ, determines how strongly the area parameter is weighted. If it is too large, ΔH will always be strongly positive, and few, if any, exchanges will occur. The volume constraint parameter can be set to a value that makes it reasonably effective in maintaining cell area if the temperature, T, is set large enough. However, if T is set too high, cells tend to dissociate, and the number of cells which are not simply connected increases. Evidently, these parameters must be assigned within a relatively narrow range for the simulations to be realistic. These

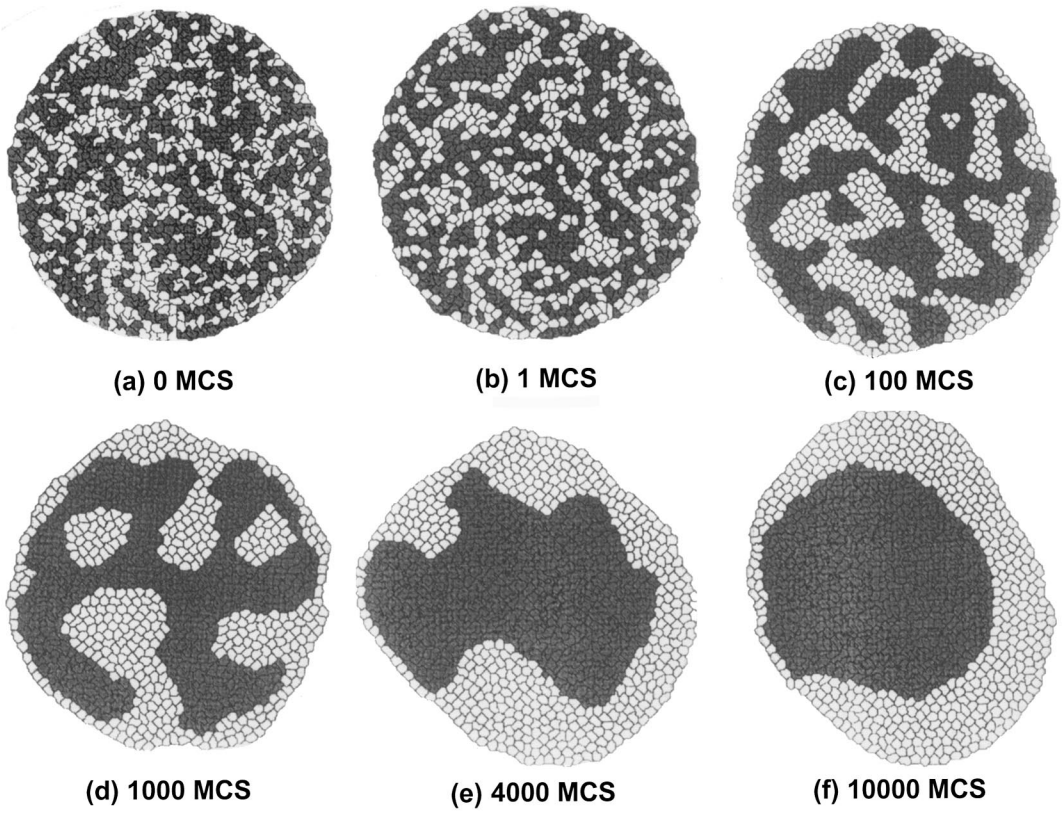

Fig. 23 Simulation of cell sorting using a sub-cellular lattice model: *a*) Initial configuration. Surface energies, which correspond directly with surface tensions, have been assigned values of $\gamma^{DD}=2$, $\gamma^{LD}=11$, $\gamma^{LL}=14$ and $\gamma^{LM}=\gamma^{DM}=16$, *b*) through *e*) Intermediate states showing the characteristic components of sorting. *f*) The final configuration. MSC is a pseudo-time parameter based on the number of Monte Carlo steps used. Sorting is explicitly predicted by the theory, but engulfment of the dark cells by the light cells is not. Reprinted from [135] with permission.

parameters have provided a powerful means of investigating the role of membrane fluctuations [144].

Another drawback of the sub-cellular lattice approach is that the cells always have jagged boundaries. This difficulty cannot be overcome by refining the mesh. For example, the length along a staircase angled at 45° will always be $\sqrt{2}$ times its diagonal length, regardless of how fine it is. Thus, a sub-cellular model cannot accurately represent the length of angled boundaries. However, as the distance between endpoints of an edge reduce, the length of the staircase between them usually also reduces. The directional nature of the fixed grid means that these methods are not frame invariant, because the length of a boundary with endpoints a certain distance apart depends on its orientation, and can vary by as much as a factor of $\sqrt{2}$. Other drawbacks of this approach include the occurrence of cells that are not simply connected and the need to find suitable values for the parameters λ and T.

In spite of these shortcomings, sub-cellular lattice models have proved highly effective in modeling a wide range of phenomena and in predicting the conditions for them (Tables 4 and 5). The simulation shown in Fig. 23 demonstrates the various aspects of cell sorting while that shown in Fig. 24 demonstrates dissociation and a number of other phenomena. A sub-cellular lattice model can represent a large number of cells (eg, $n=1000$) and can be extended to 3D without inherent difficulty [145]. However, like the other models discussed to this point, it does not model the viscosity of the cytoplasm and, therefore, cannot be directly correlated with time. It also does not model the angles between cells—perhaps the most significant drawback of this otherwise superb method.

4.6 Finite element models

The finite element method [98–100] is the newest and most complex of the methods presented in this review [46] and is one of the methods most likely to be used in the future.

Figure 25 shows a cross-section of a cell and its corresponding finite element model. Since finite element models are vertex based, they model the actual shape of a cell more closely than do other methods. In the model shown, cell edges are assumed to be straight, and each n-sided cell is broken into n triangular area elements. Finer meshes could be used if desired [146] in order to more closely accommodate the somewhat curved boundaries between cells [147]. The triangular elements are assigned a viscosity μ and are assumed to model the effective viscosity of the cell cytoplasm, its embedded networks and organelles, and any other factors that cause the cell to resist deformation [46]. For the rates of deformation characteristic of cell-cell interactions and other morphogenetic movements, this assumption seems to be appropriate. To allow cytoplasm to move freely from one triangular element to another and thereby prevent locking of the mesh, Poisson's ratio is set to zero. To then enforce constancy of cell volume, a Lagrangian side condition is imposed [46].

In applying the finite element method, each cell is broken into elements that are small enough that the behavior of the object within that element can be described by a relatively

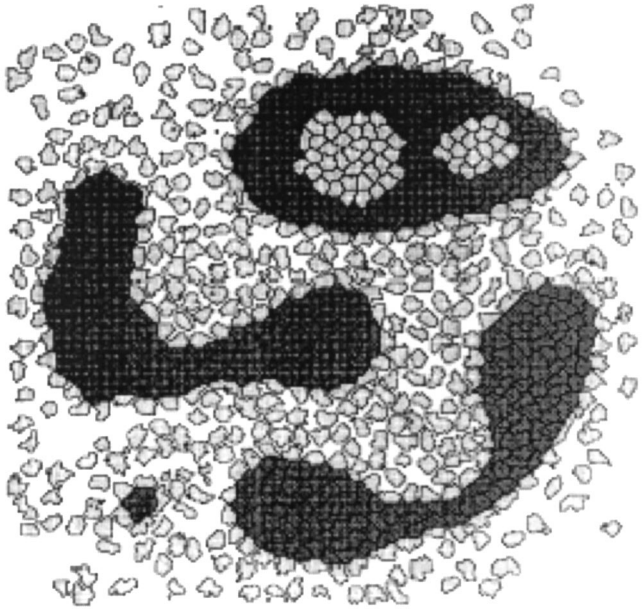

Fig. 24 Simulation of multiple interactions using a sub-cellular lattice model: The final state shown demonstrates the power of this approach to model multiple complex interactions. Here $\gamma^{DD}=4$, $\gamma^{LD}=11$, $\gamma^{LL}=14$, $\gamma^{LM}=2$, and $\gamma^{DM}=16$, and dark cells remain compact and round, while light cells in contact with the medium dissociate. (Reprinted from [27] with permission.)

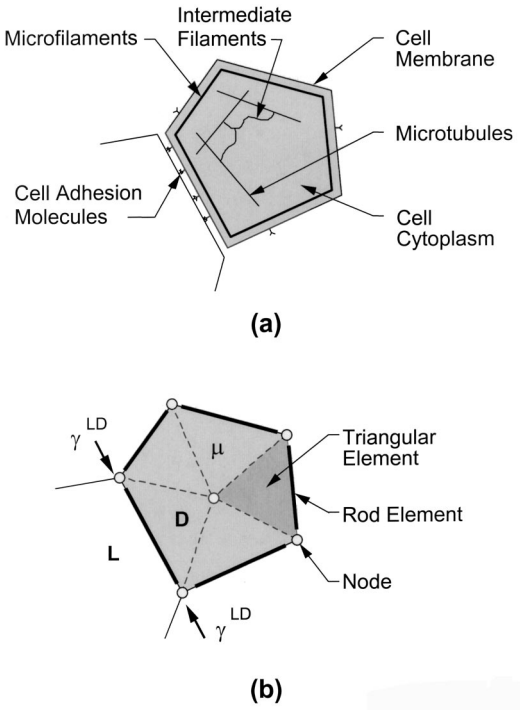

Fig. 25 Schematic cell cross-section and its corresponding finite element model: *a*) A cross-section of a typical cell. *b*) the corresponding finite element model.

straightforward mathematical expression. In the case of plane, triangular elements such as those used here (Fig. 25), the strain and strain rate are assumed to be uniform within each triangle. This assumption, or one like it for more complex element geometries, makes it possible to use variational principles or virtual work concepts to construct a stiffness matrix [98–100]. This matrix relates the forces acting at the nodes of the element to the displacements and velocities of those nodes. Matrices for each such element are then assembled to produce a global stiffness matrix **K**, which can be solved to determine the response of the system.

The interfacial tensions along each cell edge are modeled using constant force, rod-like elements along each cell boundary. Compared to standard rod elements, these have the unusual characteristic of zero stiffness. Visco-elastic properties of the cell membrane or other cell characteristics that produce non-constant forces could also be used. For any particular configuration of the aggregate, the forces generated by each boundary element are calculated and resolved into their Cartesian coordinates and assembled to produce a global force vector **f**.

During any increment of time Δt, the forces **f** generated by these boundary elements will be just matched by the forces $\mathbf{K}\Delta\mathbf{u}$ generated by the cell cytoplasm. As a result, the system of equations

$$\mathbf{K}\Delta\mathbf{u}=\mathbf{f} \tag{9}$$

can be used to calculate the incremental displacements $\Delta\mathbf{u}$ generated during the time step Δt. Constraints corresponding to fixed cell volume and boundary conditions are imposed prior to the solving of Eq. (9).

In general, the geometry of the system will change following each time step. In addition, the topology may change as short boundaries ''flip'' according to the algorithm shown in Fig. 21 [46]. The stiffness matrix **K** and driving force vector **f** are recalculated for each time step. If the cytoplasm were assumed to be viscoelastic, the calculation of the element stiffness matrix **K** would be substantially more complicated, and elastic contributions to **f** would have to be calculated based on the deformation history of the element.

This finite element procedure can be summarized as follows:

1) An initial cell configuration is generated using a Dirichlet tesselation or other means.
2) Each cell is divided into discrete finite elements. In the present model, each *n*-sided cell is broken into n triangular elements, but other subdivisions are possible.
3) All element stiffness matrices are calculated and assembled to produce a global stiffness matrix **K**. All driving forces are calculated, including those in the boundary elements, and are assembled into a global force vector **f**.
4) The equations are solved for all unknown displacements and forces (unknown elements of $\Delta\mathbf{u}$ and **f**). For each degree of freedom at each node, either the load or the displacement will be known, while the other will not be.
5) The boundary ''flip'' algorithm (Fig. 21) is applied to

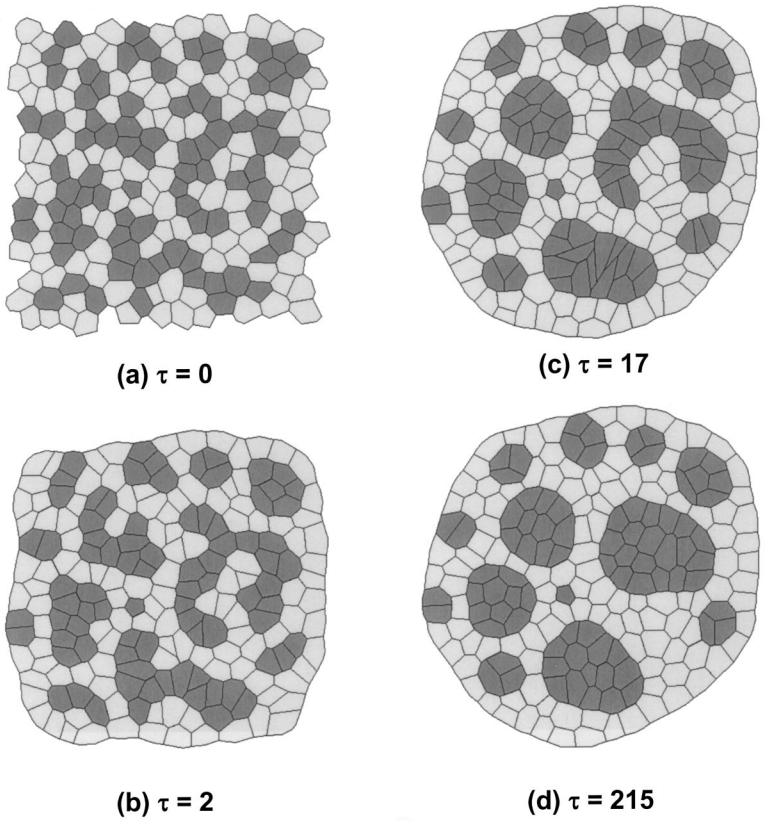

Fig. 26 Simulation of cell sorting using a finite element model: *a*) initial configuration, with $\gamma^{DD}=5$, $\gamma^{LD}=30$, $\gamma^{LL}=15$, $\gamma^{LM}=40$, and $\gamma^{DM}=60$, *b*) and *c*) intermediate states showing the characteristic components of sorting; *d*) the final configuration.

very short cell boundaries, on the basis that, if not flipped, these boundaries will probably pass through zero length during the next time step.

6) Steps 2–5 are repeated until motion stops or some other criterion is satisfied.

Figure 26 shows a finite element simulation of the interactions between two cell types. Sorting is seen to involve a number of distinguishable components [83], including the formation of chains of like cells, the shortening of these chains, the rounding of the resulting clumps and the annealing of the cells within the clumps in accordance with the criteria shown in Table 4. These sorting actions are typically accompanied by the engulfment of one cell type by the other along the edge of the aggregate in accordance with engulfment criteria (Table 5). Figure 27 shows a starting configuration and five final states that result depending on the interfacial tensions that act. Figure 28 shows a simulation of the initial stages of the dissolution of a mass, and Fig. 29 shows a simulation of engulfment. Investigations of aggregates that have more than two cell types have also been carried out [13]. These simulations demonstrate that the criteria in Tables 4 and 5 predict the interactions between each pair of cell types. Thus, cell types *A* and *B* might mix with each other, while those of type *C* might sort out from both *A* and *B*.

There are a number of advantages to using the finite element method to study cell-cell interactions. One of these advantages is that the finite element has been studied sufficiently that its mathematical and numerical properties are well known. As a result, formulations can be devised that can be trusted not to introduce errors into the solution stage of the process. In addition, the method is sufficiently general that any material properties, interactions or control variables can be accommodated. Indeed, in some of the morphogenetic problems studied using the finite element method, it has been useful and appropriate to assign negative stiffnesses to certain materials in the cell [6]. It is the only method to date that calculates the forces generated by a volume of cytoplasm that is the shape and size of that which fills each cell. As a result, it is the first method for which the simulation time

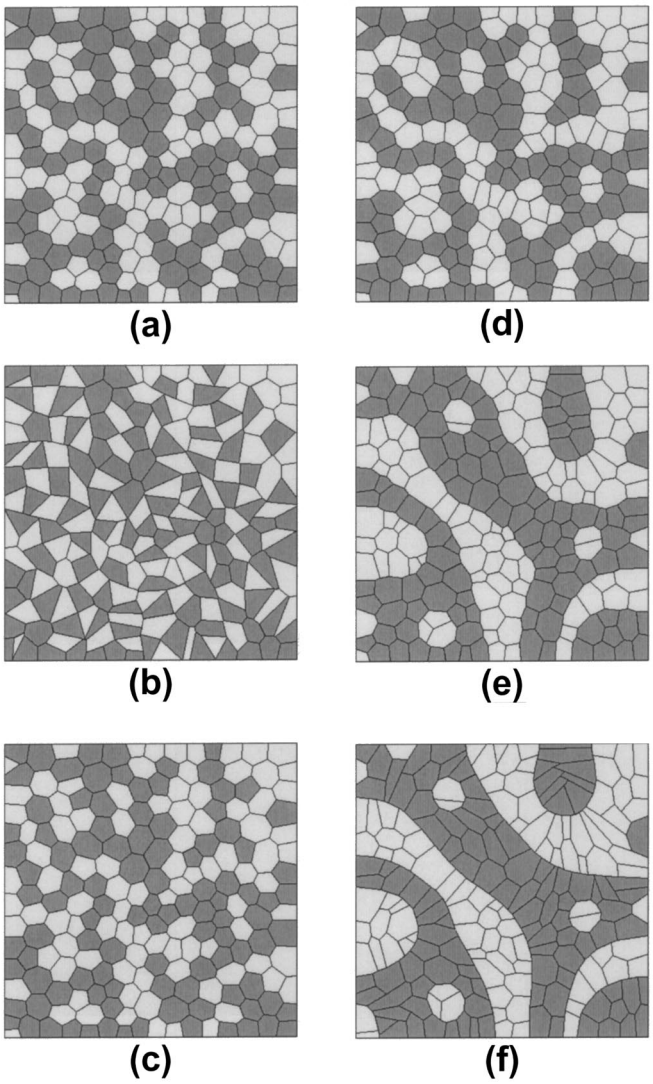

Fig. 27 Simulations showing the effect of γ^{LD}: *a*) Initial configuration with $\gamma^{LL}=12$ and $\gamma^{DD}=20$; *b*) When $\gamma^{LD}=3$, a final state demonstrating mixing, and partial checkerboarding results; *c*) When $\gamma^{LD}=14$, partial mixing occurs. *d*) When $\gamma^{LD}=22$, partial sorting occurs. *e*) When $\gamma^{LD}=40$, there is a strong tendency toward sorting, but its effect is limited by the boundary conditions. *f*) When the configuration shown in *e*) is used as a starting configuration, $\gamma^{LL}=\gamma^{DD}=0$ and $\gamma^{LD}=40$, the system of cells behaves like a system of immiscible fluids, and the boundaries between different cell types become smooth like the boundary between immiscible fluids. Reprinted from [13].

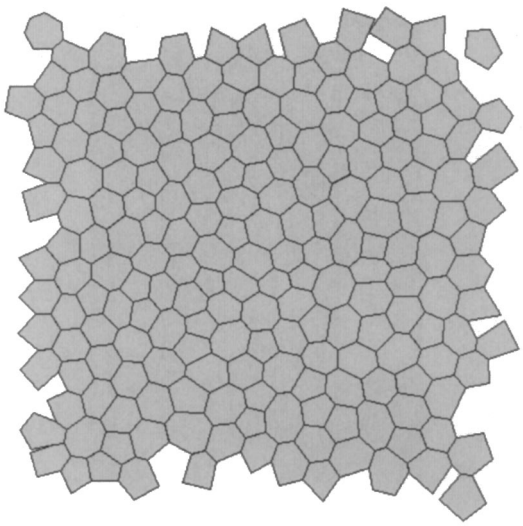

Fig. 28 Simulation of dissolution using the finite element method: When $\gamma^{LL}=30$ and $\gamma^{LM}=10$, it is energetically preferable for cells to be in contact with the medium rather than with each other. As a result, the triple junctions between pairs of cells and the medium are drawn into the mass pulling the medium in as they move. The result is that the medium infiltrates the cell-cell interfaces, causing the surface cells to dissociate from the mass. If the process were allowed to continue, the newly exposed surface cells would also dissociate from the mass until all of the cells become separated from each other.

scale corresponds to real time. Another feature of finite element simulations is that arbitrary cell shapes can be studied [46].

Unfortunately, finite element code of the kind required to study cell-cell interactions is difficult to write and debug, and commercial codes, although powerful, are missing critical features needed to study this class of problems. Finite element simulations also require much more computing power than the other methods considered in this review. It is probable, however, that ongoing advances in computing power will overcome this drawback and that finite element simulations of biological systems will become increasingly popular.

4.7 Other models

For the sake of completeness, a number of other models used to investigate cell-cell interactions are mentioned. These models include a contact and adherence model [148], a topological exchange model [149,150], and a point model with attractive and repulsive forces [151]. The paper by Matela and Fletterick [149] was the first to describe a topological mechanism for cell neighbor changes, an important component of most newer models.

Investigations into the role of cell surface proteins in sorting [42,61–66] have led to a number of new ideas that may form the basis of future theories.

5 DISCUSSION

As this article has shown, computational models have played a critical role in the advancement of the science of cell-cell interactions. They have served this role because they provide an objective and reliable way to test hypotheses about the forces that drive specific types of cell-cell interactions. Because the interactions that occur are complex, intuitive arguments are not reliable. Computational models make it possible to investigate changes to the proportions of cells present and to test how cells with any desired combination of properties would behave. They also allow the user to monitor the process by which specific phenomena occur and to study each phenomenon at any desired spatial or temporal level of detail. Thus, it becomes possible to follow the remarkable process by which force interactions that occur at triple junctions cause local motions and changes of shape that *accumulate* so as to produce actions, such as sorting, that are visible on a global scale.

Cell-cell interactions are ideally suited to investigation using computer simulations because cell properties and interaction rules can be expressed mathematically. Cell-like initial configurations can be constructed by computer, and the detailed motions of individual triple junctions, changes in cell shape and bulk motions of whole cells can be followed. In some models, the angles between cells can also be monitored. It should be emphasized that in the models considered herein, the cells are given specific properties, and the computational model then serves to demonstrate which changes in geometry or motions these properties would cause the cells in the model to undergo. It is this capability that makes computational models so well suited to testing hypotheses about the forces that drive specific rearrangements and changes in shape [6]. In some cases, combinations of actions (Figs. 23, 24, 26) occur. It is the responsibility of an observer to interpret these motions and to determine whether the final states produced have meaning, such as corresponding in part or in whole to configurations shown in Figs. 1 and 2.

Computational models of cells offer a number of important advantages compared to the physical systems that they represent. These advantages include the ability to visualize quantities, such as stresses or forces, which are invisible or impractical to measure. With appropriate software, internal regions of the model can be visualized and viewed from any angle or at any magnification, and quantities, such as those that describe cell shapes or contact angles, can be calculated on an individual or statistical basis. Models also permit multiple tests to be run from identical starting conditions. In addition, arbitrary modifications can be made to material properties, geometries, and interaction rules. Thus, it is possible to use simulations to investigate systems that may be difficult, if not impossible, to construct physically. Arbitrarily small or large changes can be made to these systems with precision and repeatability, and their effects observed.

In operating a computational model, the user specifies all of the properties and interaction rules to be used. Thus, if a test produces a certain effect, it can be known with certainty that the result was produced entirely by those encoded properties and rules. This conclusion assumes that the software is properly written and tested, and that it was operated within the bounds for which it was tested. If such is not the case, then spurious effects might be produced by faulty software or its inappropriate application.

Finally, suitable software allows the user to view the computational model results at the most beneficial rate, to review results in reverse, or to view a selected period repeatedly until it is understood. In view of these powerful features, it is not surprising that computer simulations have become a primary tool for investigating cell-cell interactions.

Fortunately, experimental data need not be complete before computational models can play a meaningful role. In-

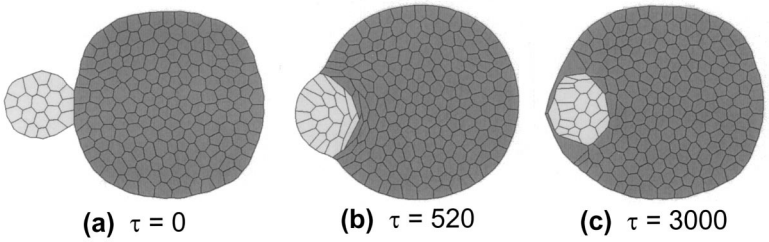

Fig. 29 Simulation of total engulfment using the finite element method: *a*) Initial configuration with $\gamma^{LL}=\gamma^{DD}=5$, $\gamma^{LD}=25$, $\gamma^{LM}=150$, $\gamma^{DM}=70$; *b*) The dark cells are drawn over the light cells; *c*) Total engulfment of the light cells by the dark cells has occurred.

deed, computer simulations based on assumed properties have often brought important insights [6,152] and provided the focus for subsequent experiments. Computational models of cell-cell interactions have often played exactly this role. Simulations based on this approach are particularly relevant in biology, where a complete set of relevant data is almost never available even for any one single cell type. Thus, it is necessary to use assumed or estimated values for some of the properties that are input to the model.

Dimensional analysis can facilitate this process in several ways. First, when results are reported in dimensionless form, they can be applied to systems having many different combinations of actual geometric and mechanical properties. Second, dimensionless findings can be used to make inferences about biological systems whenever the actual properties of that system become known in sufficient detail. Third, dimensional analysis can be very useful in identifying the parameters that govern a particular system. This approach can greatly facilitate the characterization of the real system and can substantially reduce the number of simulations that must be run to fully investigate it. In mathematical terms, this advantage is possible because dimensional analysis can reduce the dimension of the sample space that must be studied.

Computational models suggest a reason that most patterns and structures form while an embryo is small and consists of relatively few cells. Because cell-cell interactions have a neighborhood of influence of only a few cells, long periods of time would be required to organize larger masses, and the probability of errors would be much increased. The size of individual cells must remain small during these events so that the surface-to-volume ratio remains large enough that the surface properties of the cells can produce the required motions within a reasonable period of time. The computational models show that there must be an adequate imbalance in the inequality conditions in order to produce reasonable rates of motion.

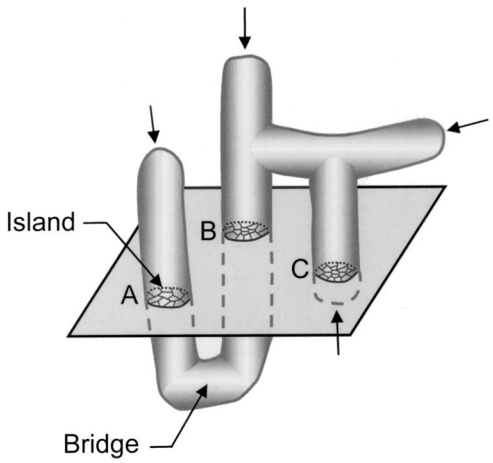

Fig. 30 Fundamental difference between two- and three-dimensional sorting. When cells form 3D aggregates, groups of like cells, *B*, in any one plane may be connected to other similar groups, such as *A* and *C*, by bridges that involve the third dimension. Interfacial tensions would act along the surfaces of these bridges and would either draw the isolated clumps together (*A* and *B*) or would draw cells out of the plane as the bridges shorten (*C*). A 2D model would not benefit from these effects, and cell sorting would be less complete in the sense that isolated groups of cells in the plane would remain isolated. Reprinted from [13].

That morphogenesis occurs by a succession of events may also have a mechanical basis. The computational models show that multiple conditions must usually be satisfied for a certain pattern of cell re-arrangement to occur. For example, engulfment of tissue *A* by tissue *B* requires not only that γ_{AM} be large enough to pull tissue *B* over *A*, but also that tissues *A* and *B* not spontaneously dissociate in the medium, and that the tissues *A* and *B* remain sorted from each other. If three or four tissues were to interact in a prespecified manner, many conditions would have to be satisfied simultaneously. Multiple kinds of independent adhesion systems may be required to satisfy these conditions, and even then, the rates of motion might be limited. Once in place, cells could be locked into position using an extra-cellular matrix (ECM) or other means.

The cell-cell interactions shown in Figs. 1 and 2 have been investigated from a wide variety of experimental, theoretical and computational perspectives. Because the findings all appear to be consistent with the DITH, this hypothesis seems to provide a unified explanation for all of these kinds of cell-cell interactions. Another benefit of the computational models that led to the DITH is that they brought focus to the relationships between cell-cell adhesion and interfacial tension.

The reversibility of cell-cell adhesion and the motility of the adhesion sites over the cell surface are two issues that warrant attention. The concept of a constant interfacial tension assumes that adhesion is thermodynamically reversible and that the adhesion sites are uniformly distributed over the contacting surfaces and fixed in location. If that were not the case, surfaces could begin to separate without breaking any bonds between adhesion sites, because the binding sites could all slide in the planes of the membranes so that they stayed inside the regions that are closely bound. These issues pose a more serious challenge to the concept of a constant surface tension. The DITH does not preclude the possibility that the effective surface tension of a surface is different when the area of contact is increasing as opposed to fixed or decreasing [13]. Thus, if effective surface tensions for all three cases can be established, the conditions for a specific phenomenon can still be written. Any rate-dependent effects can be incorporated in a similar fashion. Studies in which the strengths of the interfacial tensions are varied with time show that such variations have minimal effect. Thus, as details of cell-cell adhesion become known and any spatial or temporal variations identified, it is unlikely that these details will have a significant effect on the main concepts presented herein.

6 TOWARDS THE FUTURE

In spite of the dramatic advances that have been made, a number of significant challenges remain. One of these challenges is to develop 3D polyhedral models of cells to inves-

tigate the differences between 2D and 3D systems of cells (Fig. 30) and the specific ways that these differences might affect sorting and other phenomena [13]. It will not be difficult to represent such cells in three-dimensions and to mesh the resulting shapes. However, it may be very challenging to develop algorithms that allow such cells to rearrange in three dimensions. As a result, cell lattice and sub-cellular lattice models may be more practical for the first 3D studies.

In time, an understanding of cell-cell interactions at the sub-cellular level shown in Fig. 4 will likely be obtained. It would presumably deal with a number of open issues that are implicit in the DITH and in other hypotheses. Apparently, cell membrane is supplied to and removed from the cell surface as the triple junction moves. What are the mechanisms and kinematics of this process? Likewise, any specialized structures along the three-dimensional length of the triple junction must move or be rebuilt. There are similar questions about desmosomes and other junctions between cells, cell-adhesion molecules and other ultrastructural components. Understanding the details of cell-cell interactions at this level may require computational simulations that model individual structural components and that are fully three-dimensional. Although it may be technically feasible to construct such models now, more must first be learned from experimental investigations of the characteristics of these sub-cellular structures before the biological relevance of such models can be assured. Such models may also be able to bring insight into the intercalation of cells in epithelia [110] and other phenomena [153,154] that current models cannot adequately explain.

Another area that can be expected to develop quickly in the future is the use of computational models to determine mechanical properties. Certain cell properties can be notoriously difficult to measure, and comparison of time constants and geometric parameters between real and simulated aggregates may provide the best way to determine some of these cell properties [83,105,152].

In summary, as more becomes known about the mechanical and biochemical aspects of cell-cell interactions, computational models will be required to play an increasingly central role because of their ability to elucidate the causes of specific patterns of behavior in complex systems.

ACKNOWLEDGMENT

This work was funded by the Natural Sciences and Engineering Research Council of Canada (NSERC).

REFERENCES

[1] Cowin SC (2000), How is a tissue built?, *ASME J. Biomech. Eng.* **122**, 553–569.
[2] Nodder S and Martin P (1997), Wound healing in embryos: A review, *Anat. Embryol.* **195**, 215–228.
[3] Wijnhoven BP, Dinjens WN, and Pignatelli M (2000), E-cadherin-catenin cell-cell adhesion complex and human cancer, *Br. J. Surg.* **87**(8), 992–1005.
[4] Walgenbach KJ, Voigt M, Riabikhin AW, Andree C, Schaefer DJ, Galla TJ, and Bjorn J (2001), Tissue engineering in plastic reconstructive surgery, *Anat. Rec.* **263**(4), 372–378.
[5] Trinkaus JP (1984), *Cells Into Organs: The Forces that Shape the Embryo*, Englewood Cliffs NJ.
[6] Clausi DA and Brodland GW (1993), Mechanical evaluation of theories of neurulation using computer simulations, *Development* **118**, 1013–1023.
[7] Holmes TC (2002), Novel peptide-based biomaterial scaffolds for tissue engineering, *Trends Biotechnol.* **20**(1), 16–21.
[8] Stark GB, Volgt M, Andree C, Schaefer DJ, and Bannasch H (2000), Cell transplantation in surgery—reality and prospects for tissue engineering, *Schweiz Rundsch Med. Prax* **89**(43), 1737–1740.
[9] Turner S and Sherratt JA (2002), Intercellular adhesion and cancer invasion: A discrete simulation using the extended potts model, *J. Theor. Biol.* **216**, 85–100.
[10] Burdick MM, McCarty OJ, Jadhav S, and Konstantopoulos K (2001), Cell-cell interaction in inflammation and cancer metastasis, *IEEE Eng. Med. Biol. Mag.* **20**(3), 86–91.
[11] Steinberg MS and Foty RA (1997), Intercellular adhesions as determinants of tissue assembly and malignant invasion, *J. Cell Physiol.* **173**, 135–139.
[12] Steinberg MS (1963), Reconstruction of tissues by dissociated cells, *Science* **141**(3579), 401–408.
[13] Brodland GW (2002), The differential interfacial tension hypothesis (DITH): A comprehensive theory for the self-rearrangement of embryonic cells and tissues, *ASME J. Biomech. Eng.* **124**, 188–197.
[14] Taber LA (1995), Biomechanics of growth, remodeling, and morphogenesis, *Appl. Mech. Rev.* **48**(8), 487–545.
[15] Mackerle J (1998), A finite element bibliography for biomechanics (1987–1997), *Appl. Mech. Rev.* **51**(10), 587–634.
[16] Endy D and Brent R (2001), Modelling cellular behaviour, *Nature (London)* **409**, 391–395.
[17] Tomita M (2001), Whole-cell simulation: A grand challenge of the 21st century, *Trends Biotechnol.* **19**(6), 205–210.
[18] Brodland GW (1994), Finite element methods for developmental biology, *Int. Rev. Cytol.* **150**, 95–118.
[19] Sun E and Cohen FE (1993), Computer-assisted drug discovery—A review, *Gene* **137**(1), 127–132.
[20] Huiskes R, Ruimerman R, vanLenthe GE, and Janssen JD (2000), Effects of mechanical forces on maintenance and adaptation of form in trabecular bone, *Nature (London)* **405**, 704–706.
[21] Borah B, Gross GJ, Dufresne TE, Smith TS, Cockman MD, Chmielewski PA, Lundy MW, Hartke JR, and Sod EW (2001), Three-dimensional microimaging (MRmicroI and microCT), finite element modeling, and rapid prototyping provide unique insights into bone architecture in osteoporosis, *Anat. Rec.* **265**(2), 101–110.
[22] VanderSloten J, Hobatho MC, and Verdonck P (1998), Applications of computer modelling for the design of orthopaedic, dental and cardiovascular biomaterials, *Proc. Inst. Mech. Eng.* **212**(6), 489–500.
[23] Steinberg MS (1970), Does differential adhesion govern self-assembly processes in histogenesis? Equilibrium configurations and the emergence of a hierarchy among populations of embryonic cells, *J. Exp. Zool.* **173**, 395–434.
[24] Steinberg MS (1996), Adhesion in development: An historical overview, *Dev. Biol.* **180**, 377–388.
[25] Trinkaus JP and Lentz JP (1964), Direct observation of type-specific segregation in mixed cell aggregates, *Dev. Biol.* **9**, 115–136.
[26] Armstrong PB (1989), Cell sorting out: The self-assembly of tissues in vitro, *Crit. Rev. Biochem. Mol. Biol.* **24**(2), 119–149.
[27] Glazier JA, and Graner F (1993), Simulation of the differential adhesion driven rearrangement of biological cells, *Phys. Rev. E* **47**(3), 2128–2154.
[28] Trembley A (1744), Mémoires por servir à l'histoire d'un genre de polypes d'eau donce, à bras en forme de cornes, Jean and Herman Verbeek, Leiden.
[29] Wilson HV (1907), On some phenomena of coalescence and regeneration in sponges, *J. Exp. Zool.* **5**, 245–258.
[30] Holtfreter J (1944), Experimental studies on the development of the pronephros, *Rev. Can. Biol.* **3**, 220–250.
[31] Moscona A (1952), Cell suspensions from organ rudiments of chick embryos, *Exp. Cell Res.* **3**, 535–539.
[32] Steinberg MS (1962), On the mechanism of tissue reconstruction by dissociated cells, I: Population kinetics differential adhesiveness, and the absence of directed migration, *Zoology* **48**, 1577–1582.
[33] Steinberg MS (1962), Mechanism of tissue reconstruction by dissociated cells, II: Time-course of events, *Science* **137**, 762–763.
[34] Steinberg MS (1962), On the mechanism of tissue reconstruction by dissociated cells, III: Free energy relations and the reorganization of fused heteronomic tissue fragments, *Zoology* **48**, 1769–1776.
[35] Steinberg MS and Wiseman LL (1972), Do morphogenetic tissues rearrangements require active cell movements? *J. Cell Biol.* **55**, 606–615.
[36] Edelstein BB (1971), Cell specific diffusion model of morphogenesis, *J. Theor. Biol.* **30**, 515–532.

[37] Harris AK (1976), Is cell sorting caused by differences in the work of intercellular adhesion? A critique of the Steinberg hypothesis, *J. Theor. Biol.* **61**, 267–285.
[38] Burnside B (1971), Microtubules and microfilaments in newt neurolation, *Dev. Biol.* **26**, 416–441.
[39] Burnside B (1973), Microtubules and microfilaments in amphibian neurolation, *Am. Zool.* **13**, 989–1006.
[40] Gordon R, Goel NS, Steinberg MS, and Wiseman LL (1975), A rheological mechanism sufficient to explain the kinetics of cell sorting, *Mathematical Models for Cell Rearrangement*, Ed GD Mostow, Yale Univ Press, New Haven. (Reprinted from (1972), J. Theor. Biol. **37**, 43–73.)
[41] Goel NS, Campbell RD, Gordon R, Rosen R, Martinez H, and Ycas M (1970), Self-sorting of isotropic cells, *J. Theor. Biol.* **28**, 423–468.
[42] Friedlander DR, Mège R-M, Cunningham BA, and Edelman GM (1989), Cell sorting-out is modulated by both the specificity and amount of different cell adhesion molecules (CAMs) expressed on cell surfaces, *Proc. Natl. Acad. Sci. USA* **86**, 7043–7047.
[43] Honda H (1978), Description of cellular patterns by Dirichlet domains: The two-dimensional case, *J. Theor. Biol.* **72**, 523–543.
[44] Sulsky D, Childress S, and Percus JK (1984), A model of cell sorting, *J. Theor. Biol.* **106**, 275–301.
[45] Honda H, Yamanaka H, and Eguchi G (1986), Transformation of a polygonal cellular pattern during sexual maturation of the avian oviduct epithelium: Computer simulation, *J. Embryol. Exp. Morphol.* **98**, 1–19.
[46] Chen HH and Brodland GW (2000), Cell-level finite element studies of viscous cells in planar aggregates, *ASME J. Biomech. Eng.* **122**, 394–401.
[47] Issajew W (1926), Studien an organischen regulationen (experimentalle untersuchungen an hydren), *Roux Archive Entwicklungsmechanik* **108**, 1–67.
[48] Noda K (1971), Reconstitution of dissociated cells of hydra, *Zool. Mag.* **80**, 99–101. ISSN004-5118
[49] Bode PM and Bode HR (1984), Formation of pattern in regenerating tissue pieces of Hydra attenuata, III: The shaping of the body column, *Dev. Biol.* **106**, 315–325.
[50] Rieu JP, Kataoka N, and Sawada Y (1998), Quantitative analysis of cell motion during sorting in two-dimensional aggregates of dissociated hydra cells, *Phys. Rev. E* **57**(1), 924–931.
[51] Technau U and Holstein TW (1992), Cell sorting during the regeneration of hydra from reaggregated cells, *Dev. Biol.* **151**, 117–127.
[52] Alberts B, Bray D, Lewis J, Raff M, Roberts K, and Watson JD (1989), *Molecular Biology of the Cell 2nd Edition*, Garland Publishing, New York.
[53] Alberts B, Bray D, Johnson A, Lewis J, Raff M, Roberts K, and Walter P (1998), *Essential Cell Biology*, Garland Publishing, New York.
[54] Pollack GH (2001), *Cells, Gels and the Engines of Life*, Ebner and Sons, Seattle, USA.
[55] Opas M (1995), Cellular adhesiveness, contractility, and traction: Stick, grip, and slip control, *Biochem. Cell Biol.* **73**, 311–316.
[56] Ruoslahti E and Obrink B (1996), Common principles in cell adhesion, *Exp. Cell Res.* **227**, 1–11.
[57] Gumbiner BM (1996), Cell adhesion: The molecular basis of tissue architecture and morphogenesis, *Cell* **84**, 345–357.
[58] Aplin AE, Howe AK, and Juliano RL (1999), Cell adhesion molecules, signal transduction and cell growth, *Curr. Opin. Cell Biol.* **11**, 737–744.
[59] Petruzzelli L, Takami M, and Humes HD (1999), Structure and function of cell adhesion molecules, *Am. J. Med.* **106**, 467–476.
[60] Zhu C (2000), Kinetics and mechanics of cell adhesion, *J. Biomech.* **33**, 23–33.
[61] Armstrong PB and Armstrong MT (1984), A role for fibronectin in cell sorting, *J. Cell. Sci.* **69**, 179–197.
[62] Takeichi M, Hatta K, and Nagafuchi A (1985), Selective cell adhesion mechanism: Role of the calcium-dependent cell adhesion system, *Molecular Determinants of Animal Form*, GM Edelman (ed), AR Liss, New York, 223–233.
[63] Ohmori T and Maeda Y (1986), Implications of differential chemotaxis and cohesiveness for cell sorting in the development of *Dictyostelium discoideum*, *Dev., Growth Differ.* **28**(2), 169–175.
[64] Nose A, Nagafuchi A, and Takeichi M (1988), Expressed recombinant cadherins mediate cell sorting in model systems, *Cell* **54**, 993–1001.
[65] Steinberg MS and Takeichi M (1994), Experimental specification of cell sorting, tissue spreading, and specific spatial patterning by quantitative differences in cadherin expression, *Dev. Biol.* **91**, 206–209.
[66] Xu Q, Millitzer G, Robinson V, and Wilkinson DG (1999), *In vivo* cell sorting in complementary segmental domains mediated by Eph receptors and ephrins, *Nature (London)* **399**, 267–271.
[67] Davies JT and Rideal EK (1963), *Interfacial Phenomena*, Academic Press 2nd Edition, 1–55.
[68] Somers SD, Whisnant CC, and Adams DO (1986), Quantification of the strength of cell-cell adhesion: The capture of tumour cells by activated marine macrophages proceeds through two distinct stages, *J. Immunol.* **136**(4), 1490–1496.
[69] Umbreit J and Roseman S (1975), A requirement for reversible binding between aggregating embryonic cells before stable adhesion, *J. Biol. Chem.* **250**(24), 9360–9368.
[70] Loster K, Schuler C, Heidrich C, Horstkorte R, and Reutter W (1997), Quantification of cell-matrix and cell-cell adhesion using horseradish peroxidase, *Academic Press, Analytical Biochemistry* **244**, 96–102.
[71] Sagvolden G, Giaever E, Pettersen EO, and Feder J (1999), Cell adhesion force microscopy, *Proc. Natl. Acad. Sci. U.S.A.* **96**, 471–476.
[72] Dong C and Lei XX (2000), Biomechanics of cell rolling: Shear flow, cell-surface adhesion, and cell deformability, *J. Biomech.* **33**(1), 35–43.
[73] Masui M and Kominami T (2001), Change in the adhesive properties of blastomeres during early cleavage stages in sea urchin embryo, *Dev., Growth Differ.* **43**, 43–53.
[74] Baker PC (1965), Fine structure and morphogenic movements in the gastrula of the treefrog *Hyla Regilla*, *J. Cell Biol.* **24**, 95–116.
[75] Karfunkel P (1971), The role of microtubules and microfilaments in neurulation in xenopus, *Dev. Biol.* **25**(1), 30–56.
[76] Spooner BS and Wessells NK (1972), An analysis of salivary gland morphogenesis: Role of cytoplasmic microfilaments and microtubules, *Dev. Biol.* **27**(1), 38–54.
[77] Gershon ND, Porter KR, and Trus BL (1985), The cytoplasmic matrix: Its volumes and surface area and the diffusion of molecules through it, *Proc. Natl. Acad. Sci. U.S.A.* **82**(15), 5030–5034.
[78] Goodsell DS (1991), Inside a living cell, *Trends Biotechnol.* **16**(6), 206–210.
[79] Brodland GW and Gordon R (1990), Intermediate filaments may prevent buckling of compressively loaded microtubules, *ASME J. Biomech. Eng.* **112**, 319–321.
[80] Carraway KL and Carraway CAC (2000), *Cytoskeleton: Signalling and Cell Regulation*, Oxford Univ Press.
[81] Kuhn TS (1962), *The Structure of Scientific Revolutions 2nd Edition*, Univ of Chicago Press, Chicago IL.
[82] Brodland GW and Chen HH (2000), The mechanics of cell sorting and envelopment, *J. Biomech.* **33**, 845–851.
[83] Brodland GW and Chen HH (2000), The mechanics of heterotypic cell aggregates: Insights from computer simulations, *ASME J. Biomech. Eng.* **122**, 402–407.
[84] Foty RA and Steinberg MS (1995), *Liquid Properties of Living Cell Aggregates: Measurement and Morphogenetic Significance of Tissue Interfacial Tensions*, World Scientific Publ., 63–73.
[85] Foty RA, Pfleger CM, Forgacs G, and Steinberg MS (1996), Surface tensions of embryonic tissues predict their mutual envelopment behavior, *Development* **122**, 1611–1620.
[86] Moscona A (1957), Development in vitro of chimeric aggregates of dissociated embryonic chick and mouse cells, *Proc. Natl. Acad. Sci. U.S.A.* **43**, 184–194.
[87] Trinkaus JP and Groves PW (1955), Differentiation in culture of mixed aggregates of dissociated tissue cells, *Proc. Natl. Acad. Sci. U.S.A.* **41**, 787–795.
[88] Townes PL and Holtfreter J (1955), Directed movements and selective adhesion of embryonic amphibian cells, *J. Exp. Zool.* **128**, 53–120.
[89] Steinberg MS (1975), Adhesion-guided multicellular assembly: A commentary upon the postulates, real and imaged, of the differential adhesion hypothesis, with special attention to computer simulations of cell sorting, *J. Theor. Biol.* **55**, 431–443.
[90] Phillips HM and Steinberg MS (1969), Equilibrium measurements of embryonic chick cell adhesiveness, I: Shape equilibrium in centrifugal fields, *Proc. Natl. Acad. Sci. U.S.A.* **64**, 121–127.
[91] Foty RA, Forgacs G, Pfleger CM, and Steinberg MS (1994), Liquid properties of embryonic tissues: Measurement of interfacial tensions, *Phys. Rev. Lett.* **72**(14), 2298–3001.
[92] Beysens DA, Forgacs G, and Glazier JA (2000), Cell sorting is analogous to phase ordering in fluids, *PNAS* **97**(17), 9467–9471.
[93] Adam NK (1941, reprinted in 1968), *The Physics and Chemistry of Surfaces*, Dover Publications, New York.
[94] Armstrong PB and Parenti D (1972), Cell sorting in the presence of cytochalasin B, *J. Cell Biol.* **55**(3), 542–553.
[95] Forgacs G (1995), Biological specificity and measurable physical properties of cell surface receptors and their possible role in signal

transduction through the cytoskeleton, Biochem., *Cell Biol.* **73**(7–8), 317–26.
[96] Moscona AA (1960), Patterns and mechanisms of tissue reconstruction from dissoniated cells, *Developing Cell Systems and Their Control*, Academic Press, 45–70.
[97] Marrs JA and Nelson WJ (1996), Cadherin cell adhesion molecules in differentiation and embryogenesis, *Int. Rev. Cytol.* **165**, 159–205.
[98] Zienkiewicz, OC and Taylor RL (1988), *The Finite Element Method, 4th Edition*, Vol 1, McGraw-Hill Book Co, London, England.
[99] Crisfield MA (1991), *Non-linear Finite Element Analysis of Solids and Structures*, Vol 1, John Wiley and Sons, Chichester, England.
[100] MacNeal R (2000), *Finite Elements: Their Design and Performance*, Marcel Dekker, New York.
[101] Honda H (1983), Geometrical models for cells in tissues, *Int. Rev. Cytol.* **81**, 191–248.
[102] Armstrong PB and Armstrong MT (1990), An instructive role for the interstitial matrix in tissue patterning: Tissue segregation and intercellular invasion, *J. Cell Biol.* **110**(4), 1439–1455.
[103] Elton RA and Tickle CA(1971), The analysis of spatial distributions in mixed cell populations: A statistical method for detecting sorting out, *J. Embryol. Exp. Morphol.* **26**(1), 135–156.
[104] Ide H, Wada N, and Uchiyama K (1993), Sorting out of cells from different parts and stages of the chick limb bud, *Dev. Biol.* **162**, 71–76.
[105] Mochizuki A, Wada N, Ide H, and Iwasa Y (1998), Cell-cell adhesion in limb-formation, estimated from photographs of cell sorting experiments based on a spatial stochastic model, *Dev. Dyn.* **211**, 204–214.
[106] Honda H (1973), Pattern formation of the coenobial algae *Pediastrum biwae* negoro, *J. Theor. Biol.* **42**, 461–481.
[107] Yoshida A and Aoki K (1989), Scale arrangement pattern in lepidopteran wing, I: Periodic cellular pattern in the pupal wing of *Pieris rapae.*, *Dev., Growth Differ.* **31**(6), 601–609.
[108] Yamanaka H and Honda H (1990), A checkerboard pattern manifested by the oviduct epithelium of the Japanese quail, *Int. J. Dev. Biol.* **34**, 377–383.
[109] Yamanaka H (1990), Pattern formation in the epithelium of the oviduct of Japanese quail, *Int. J. Dev. Biol.* **34**, 385–390.
[110] Elul T and Keller R (2000), Monopolar protrusive activity: A new morphogenic cell behavior in the neural plate dependent on vertical interactions with the mesoderm in xenopus, *Dev. Biol.* **224**, 3–19.
[111] Harris AK (1999), A dozen questions about how tissue cells crawl, *Cell Behaviour: Control and Mechanism of Motility*, JM Lackie, GA Dunn, and GE Jones (eds), Princeton Univ Press, Princeton NJ, 315–341.
[112] Phillips HM, Steinberg MS, and Lipton BH (1977), Embryonic tissues as elasticoviscous liquids, II: Direct evidence for cell slippage in centrifuged aggregates, *Dev. Biol.* **59**, 124–134.
[113] Phillips HM and Davis GS (1978), Liquid-tissue mechanics in amphibian gastrulation: Germ-layer assembly in *Rana Pipiens*, *Am. Zool.* **18**, 81–93.
[114] Honda H and Eguchi G (1980), How much does the cell boundary contract in a monolayered cell sheet?, *J. Theor. Biol.* **84**, 575–588.
[115] Herbst C (1900), Uber das auseinandergehen von furchungs—und gewebezellen in kalkfreien medium, *Arch. f. Entwicklungsmech. Organ.* **9**, 424–463.
[116] Phillips HM and Steinberg MS (1978), Embryonic tissues as elasticoviscous liquids, I: Rapid and slow shape changes in centrifuged cell aggregates, *J. Cell. Sci.* **30**, 1–20.
[117] Heintzelman KF, Phillips HM, and Davis GS (1978), Liquid-tissue behavior and differential cohesiveness during chick limb budding, *J. Embryol. Exp. Morphol.* **47**, 1.
[118] Torza S and Mason SG (1969), Coalescent of two immiscible liquid drops, *Science* **163**, 813–814.
[119] Torza S and Mason SG (1970), Three-phase interactions in shear and electrical fields, *J. Colloid Interface Sci.* **33**(1), 67–83.
[120] Bresch D (1955), Recherches preliminaires sur des associations d'organes embryonnaires de poulet en culture in vitro, *Bull. Biol. Fr. Belg.* **89**, 179–188.
[121] Galtsoff PS (1925), Regeneration after dissociation (an experimental study on sponges), I: Behavior of dissociated cells of *Microciona prolifera* under normal and abnormal conditions, *J. Exp. Zool.* **42**, 183–221.
[122] Humphries T (1963), Chemical dissolution and in vitro reconstruction of sponge cell adhesions, I: Isolation and functional demonstration of the components involved, *Dev. Biol.* **8**, 27–47.
[123] Humphries T (1994), Rapid allogeneic recognition in the marine sponge *Microciona prolifera*: Implications for evolution of immune recognition, *Ann. N.Y. Acad. Sci.* **712**, 342–345.
[124] Weiss P and James R (1955), Skin metaplasia in vitro induced by brief exposure to vitamin A, *Exp. Cell Res.* **53**, 381–394.
[125] Trinkaus JP and Gross MC (1961), The use of tritiated thymidine for marking migratory cells, *Exp. Cell Res.* **24**, 52–57.
[126] Collares-Buzato CB, Jepson MA, McEwan GTA, Hirst BH, and Simmons NL (1998), Co-culture of two MDCK strains with distinct junctional protein expression: A model for intercellular junction rearrangement and cell sorting, *Cell Tissue Res.* **291**, 267–276.
[127] Adams CL, Chen Y-T, Smith SJ, and Nelson WJ (1998), Mechanisms of epithelial cell-cell adhesion and cell compaction revealed by high-resolution tracking of E-Cadherin-green fluorescent protein, *J. Cell Biol.* **142**(4), 1105–1119.
[128] Ryan PL, Foty RA, Kohn J, and Steinberg MS (2001), Tissue spreading on implantable substrates is a competitive outcome of cell-cell vs cell-substratum adhesivity, *PNAS* **98**(8), 4323–4327.
[129] Steinberg MS (1964), The problem of adhesive selectivity in cellular interactions, *Cellular Membranes in Development*, M Locke (ed), Academic Press, New York, 321–366.
[130] Antonelli PL, Rogers TD, and Willard MA (1973), Geometry and the exchange principle in cell aggregation kinetics, *J. Theor. Biol.* **41**, 1–21.
[131] Goel NS and Rogers G (1978), Computer simulation of engulfment and other movements of embryonic tissues, *J. Theor. Biol.* **78**, 103–140.
[132] Rogers G and Goel NS (1978), Computer simulation of cellular movements: Cell-sorting, cellular migration through a mass of cells and contract inhibition, *J. Theor. Biol.* **78**, 141–166.
[133] Mochizuki A, Iwasa Y, and Takeda Y (1996), A stochastic model for cell sorting and measuring cell-cell adhesion, *J. Theor. Biol.* **179**, 129–146.
[134] Graner F and Sawada Y (1993), Can surface adhesion drive cell rearrangements? Part I: Biological cell-sorting, *J. Theor. Biol.* **164**, 455–476.
[135] Graner F and Glazier JA (1992), Simulation of biological cell sorting using a two-dimensional extended Potts model, *Phys. Rev. Lett.* **69**(13), 2013–2016.
[136] Vasiliev AB, Pyatetskii-Shapiro II, and Radvogin YB (1972), Modeling of the processes of sorting out, invasion, and aggregation of cells, *Sov. J. Dev. Biol.* **2**, 286–291.
[137] Antonelli P, McLaren DI, Rogers TD, Lathrop M, and Willard MA (1975), Transitivity, pattern reversal, engulfment, and duality in exchange-type cell aggregation kinetics, *Mathematical Models for Cell Rearrangement*, GD Mostow (ed), Yale Univ Press, New Haven and London.
[138] Mostow GD (ed), (1975), *Mathematical Models for Cell Rearrangement*, Yale Univ Press, New Haven and London.
[139] Leith AG and Goel NS (1971), Simulation of movement of cells during self-sorting, *J. Theor. Biol.* **33**, 171–188.
[140] Green PJ and Sibson R (1977), Computing dirichlet tesselations in the plane, *Comput. J. (UK)* **21**(2), 168–173.
[141] Chen HH (1998), Finite element-based computer simulation of motility, sorting, and deformation in biological cells, PhD Thesis, Univ of Waterloo, Waterloo, Canada.
[142] Hogeweg P (2000), Evolving mechanisms of morphogenesis: On the interplay between differential adhesion and cell differentiation, *J. Theor. Biol.* **203**, 317–333.
[143] Maree AFM and Hogeweg P (2002), How amoeboids self-organize into a fruiting body: Multicellular coordination in *Dictyostelium discoideum*, *Proc of National Academy of Sciences*, **98**(7), 3879–3883.
[144] Mombach JCM, Glazier JA, Raphael RC, and Zajac M (1995), Quantitative comparison between differential adhesion models and cell sorting in the presence and absence of fluctuations, *Phys. Rev. Lett.* **75**(11), 2244–2247.
[145] Glazier JA, Raphael RC, Graner F, and Sawada Y (1995), The energetics of cell sorting in 3 dimensions, *Interplay of Genetic and Physical Processes in the Development of Biological Form*, D Beysens, G Forgacs, and F Gaill (eds), World Scientific, Singapore, 54–61.
[146] Breuls RG, Sengers BG, Oomens CW, Bouten CV, and Baaijens FP (2002), Predicting local cell deformations in engineered tissue constructs: A multilevel finite element approach, *ASME J. Biomech. Eng.* **124**, 198–207.
[147] Stein MB and Gordon R (1982), Epithelia as bubble rafts: A new method for analysis of cell shape and intercellular adhesion in embryonic and other epithelia, *J. Theor. Biol.* **97**, 625–639.
[148] Rogers TD and Sampson JR (1977), A random walk model of cellular kinetics, *Int. J. Bio-Med. Comput.* **8**(1), 45–60.
[149] Matela RJ and Fletterick RJ (1979), A topological exchange model for cell self-sorting, *J. Theor. Biol.* **76**, 403–414.
[150] Matela RJ and Fletterick RJ (1980), Computer simulation of cellular

cell-sorting: A topological exchange model, *J. Theor. Biol.* **84**, 673–690.
[151] Greenspan D (1981), A classical molecular approach to computer simulation of biological sorting, *J. Math. Biol.* **12**, 227–235.
[152] Davidson LA, Koehl MAR, Keller R, and Oster GF (1995), How do sea urchins invaginate? Using biomechanics to distinguish between mechanisms of primary invagination, *Drug Metab. Rev.* **121**, 2005–2018.
[153] Mombach JCM and Glazier JA (1996), Single cell motion in aggregates of embryonic cells, *Phys. Rev. Lett.* **76**(16), 3032–3035.
[154] Gail MH and Boone CW (1970), The locomotion of mouse fibroblasts in tissue culture, *Biophys. J.* **10**, 980–993.

G Wayne Brodland *is Professor of Civil Engineering at the University of Waterloo. He holds degrees in Mechanical, Biomedical, and Civil Engineering, the most recent being a PhD in Civil Engineering from the University of Manitoba in 1985. He and his research group use analytical, computational, and experimental approaches to investigate embryo morphogenesis including cell-level interactions like those reviewed in this article. They are especially interested in morphogenesis of the neural tube, the precursor of the spinal cord and brain, because irregularities in this process give rise to spina bifida, the most common of human birth defects. They have built several computer-controlled microscopes and written extensive software to make three-dimensional reconstructions of live amphibian embryos and to analyze the detailed kinematics of morphogenetic processes. Their research has been funded by NSERC, CIHR, The Easter Seals Research Institute (ESRI), the Spina Bifida and Hydrocephalus Association of Canada (SBHAC), and private industry.*